SECURITY INFORMATION

CONFIDENTIAL

Copy 397
RM L53D14

NACA RM L53D14

NACA

RESEARCH MEMORANDUM

PRELIMINARY INVESTIGATION OF THE EFFECT OF FENCES AND BALANCING TABS ON THE HINGE-MOMENT CHARACTERISTICS OF A TIP CONTROL ON A 60° DELTA WING AT MACH NUMBER 1.61

By K. R. Czarnecki and Douglas R. Lord

Langley Aeronautical Laboratory
Langley Field, Va.

CLASSIFICATION CHANGED TO UNCLASSIFIED
AUTHORITY: NASA PUBLICATIONS ANNOUNCEMENT NO. 7
EFFECTIVE DATE: MAY 29, 1959
THM

CLASSIFIED DOCUMENT

This material contains information affecting the National Defense of the United States within the meaning of the espionage laws, Title 18, U.S.C., Secs. 793 and 794, the transmission or revelation of which in any manner to an unauthorized person is prohibited by law.

NATIONAL ADVISORY COMMITTEE FOR AERONAUTICS

WASHINGTON

May 29, 1953

CONFIDENTIAL

NATIONAL ADVISORY COMMITTEE FOR AERONAUTICS

RESEARCH MEMORANDUM

PRELIMINARY INVESTIGATION OF THE EFFECT OF FENCES AND BALANCING TABS ON THE HINGE-MOMENT CHARACTERISTICS OF A TIP CONTROL ON A 60° DELTA WING AT MACH NUMBER 1.61

By K. R. Czarnecki and Douglas R. Lord

SUMMARY

An investigation has been made at a Mach number of 1.61 and a Reynolds number of 4.2×10^6 of the effects of chordwise fences and attached tabs on the hinge-moment characteristics of a half-delta tip control mounted on a 60° delta wing. Tests were made over an angle-of-attack range from -12° to 12° and a control-deflection range from -30° to 30°.

Results of the investigation indicate that, in general, the effect of fences was to improve the linearity of the hinge-moment curves and to increase the negative values of the slope parameters of hinge moment against control deflection and angle of attack. Results of the tab investigation indicate that only a large tab had sufficient effectiveness in reducing control hinge moment to be of practical use and then only when relatively small maximum control deflections are permissible. A comparison of the experimental contribution of the tab to the control hinge-moment coefficients with that predicted by an approximate theory, which did not account for viscous effects, showed poor agreement.

INTRODUCTION

Tip controls have been proposed for use on delta wings at supersonic speeds in order to reduce the hinge moments without adversely affecting the control effectiveness. In contemplating the use of such control surfaces, the question arises as to the effect of placing a fence at the parting line between the wing and the control. An exploratory investigation of such a fence was reported in reference 1. It is also of interest to determine whether balancing tabs will be of any benefit at supersonic speeds. Transonic tests of balancing tabs have been reported in reference 2.

As part of a general program of research on controls an investigation is underway in the Langley 4- by 4-foot supersonic pressure tunnel to determine the important parameters in the design of controls for use on a delta wing at supersonic speeds. The first results of the tests, reported in reference 3, showed the effect of control plan form and hinge-line location on the hinge-moment characteristics for a series of tip controls on a 60° delta wing at a Mach number of 1.61.

Further tests have been made to determine the effect of fences, placed at the parting line between the wing and control, on the hinge-moment characteristics for a tip control having approximately one-fourth of its area ahead of the hinge line. Tests have also been made on the same tip control to determine the usefulness of attached tabs for reducing the control hinge moments. The results of these tests are presented in this paper, together with a theoretical analysis of the effect of attached tabs on the control hinge-moment coefficients.

All tests were made using a 60° sweptback half-delta wing with a half-delta tip control. The wing angle-of-attack range was from -12° to 12° and the control-deflection range, relative to the wing, was from -30° to 30°. The tests were conducted at a Mach number of 1.61 and at a Reynolds number of 4.2×10^{6}, based on the wing mean aerodynamic chord of 12.10 inches.

The hinge moments were measured directly by means of strain gages and the control effectiveness, by means of pressure distributions. In order to expedite the publication of the fence results, only control hinge-moment characteristics will be presented in this paper since considerable time is required for the reduction of the pressure data. Lack of orifices on the tabs prohibits the evaluation of the effectiveness of the control with the tabs.

SYMBOLS

M Mach number

q dynamic pressure

α wing angle of attack

δ control deflection relative to wing (positive when control trailing edge is deflected down)

δ_T tab deflection relative to control (positive when tab trailing edge is deflected down)

S control plan-form area (excluding tab, except where noted)

S_B control plan-form area ahead of hinge line

$\bar{c}$ control mean aerodynamic chord (excluding tab, except where noted)

H control hinge moment about hinge line

C_h control hinge-moment coefficient, $H/qS\bar{c}$

ΔC_h increment in control hinge-moment coefficient due to presence of tab

Slope parameters:

$$C_{h_\alpha} = \frac{\partial C_h}{\partial \alpha}$$

$$C_{h_\delta} = \frac{\partial C_h}{\partial \delta}$$

$$C_{h_{\delta_T}} = \frac{\partial C_h}{\partial \delta_T}$$

$$\frac{\delta_T}{\delta} = -\frac{C_{h_\delta}}{C_{h_{\delta_T}}}$$

$$\Delta C_{h_\alpha} = \frac{\partial \Delta C_h}{\partial \alpha}$$

$$\Delta C_{h_\delta} = \frac{\partial \Delta C_h}{\partial \delta}$$

$$\Delta C_{h_{\delta_T}} = \frac{\partial \Delta C_h}{\partial \delta_T}$$

All slopes were obtained at $\alpha = 0^\circ$, $\delta = 0^\circ$, $\delta_T = 0^\circ$, as applicable.

APPARATUS

Wind Tunnel

This investigation was conducted in the Langley 4- by 4-foot supersonic pressure tunnel which is a rectangular, closed-throat, single-return type of wind tunnel with provisions for the control of the pressure, temperature, and humidity of the enclosed air.

For the tests reported herein, the nozzle walls were set for a Mach number of 1.6. At this Mach number, the test section has a width of 4.5 feet and a height of 4.4 feet. During the tests, the stagnation pressure was held at 15 pounds per square inch absolute and the dewpoint was kept below -20° F so that the effects of water condensation in the supersonic nozzle were negligible.

Model and Model Mounting

The model used in this investigation consisted of a half-delta wing with a half-delta tip control surface having approximately one-fourth of its area ahead of the hinge line (configuration E in ref. 3). The model was modified during the various phases of the tests by the addition of two types of fences and two sizes of attached tabs. A sketch of the basic wing, the fences, and the tabs is shown in figure 1. Photographs showing typical installations of the modified fence and of the large tab are presented in figure 2.

The basic wing had a 60° sweptback leading edge, a root chord of 18.143 inches, and a semispan of 10.475 inches. The wing had a blunt NACA 63-series nose section extending 30 percent root chord back from the leading edge, a constant-thickness center section with a thickness ratio of 3 percent based on the root chord, and a sharp trailing edge. On the control surface, there was no constant-thickness midsection, the nose section joining directly with the tapered trailing edge.

The full-chord fence was designed to close the angular gap between the wing and the tip control due to the unporting of the control for a control-deflection range of $\pm 30^{\circ}$. The modified fence was made by cutting down the full-chord fence so that only the angular gap ahead of the hinge line was closed. Both fences were attached directly to the wing. The basic wing and control were constructed of steel. (For details of construction, see ref. 3.) The fences and tabs were made from $\frac{1}{16}$-inch stock brass.

The semispan control wing was mounted horizontally in the tunnel from a turntable in a steel boundary-layer bypass plate which was located vertically in the test section about 10 inches from the side wall as shown in figure 3.

TECHNIQUES AND TESTS

The model angle of attack was changed by rotating the turntable in the bypass plate (see fig. 3). The angle of attack was measured by a vernier on the outside of the tunnel, since the angular deflection of the wing and support under load was negligible. Control deflection was changed by a gear mechanism mounted on the pressure box which rotated the strain-gage balance, torque tube, and control as a unit. The control angles were set approximately with the aid of an electrical control-position indicator mounted on the torque tube close to the wing root and measured under load during testing with a cathetometer mounted outside the tunnel.

Control hinge moments were determined by means of an electrical strain-gage balance located in the pressure box (fig. 3) which measured the torque on the tube actuating the control surface. During some of the tests, when the control was highly loaded, friction difficulties were experienced in obtaining hinge moments. Checks for friction were made throughout the tests and, whenever friction was manifest, check points were obtained by approaching control settings from both directions and friction effects were then eliminated by averaging the two resulting curves. Checks of this method of correcting for friction results obtained when friction was not present (see ref. 3) indicated excellent agreement.

Tests were made over a wing angle-of-attack range from -12° to 12° in increments of 6°. The control-deflection range was from -30° to 30°, usually in increments of about 5°. Near control deflection of 0° this increment was reduced to about 2° or 3°. The large tab was tested at tab deflections of 1.1°, -9.3°, and -19.3°, whereas the small tab was tested at a tab deflection of -10.8° only. All tests were made at a tunnel stagnation pressure of 15 pounds per square inch corresponding to a Reynolds number of 4.2×10^{6}, based on the wing mean aerodynamic chord.

PRECISION OF DATA

The mean Mach number in the region occupied by the model is estimated from calibration to be 1.61 with local variations being smaller than ± 0.02. There is no evidence of any significant flow angularities.

The estimated accuracy of other pertinent quantities is

α, deg	± 0.05
δ, deg	± 0.1
δ_T, deg	± 0.1
C_h (corrected for friction)	± 0.005

THEORETICAL CALCULATIONS

The theoretical hinge-moment characteristics of the tip control and attached tabs were obtained by means of linearized supersonic theory except for the parameters ΔC_{h_δ} and ΔC_{h_α}. For these parameters, because of the labor involved in obtaining expressions based on linear theory, some approximate equations were derived using linear supersonic theory as a basis. Details of the derivations for the increments in control hinge moment due to the tab as a result of tab, control, and wing deflection are presented in the appendix.

RESULTS AND DISCUSSION

Effect of Fences

Hinge moments.- The variation of control hinge-moment coefficient with control deflection for the full-chord fence and modified fence configurations is presented in figure 4. In order to show the effect of the fences, the variation of hinge-moment coefficient with control deflection for the basic control configuration without fences is included in figure 4.

The most important effect of the fences was the increased linearity of the curves near 0° control deflection at angles of attack where the hinge-moment curves for the basic configuration without fences tended to be nonlinear (α near 12°). From the tests of reference 3 it was found that for more closely balanced controls, the tendency for nonlinearities and for regions of overbalance at all angles of attack was much greater. It seems, therefore, that some type of fences, when used in conjunction with a closely balanced control, would have a very desirable linearizing effect on the control hinge-moment curve. Such an effect has been found in reference 1, where the fence used was somewhat smaller than the full-chord fence used in the subject tests.

Another important effect was that the full-chord fence (fig. 4(a)) caused a general increase in slope of the curves of hinge-moment coefficient against control deflection at moderate control deflections at all

test angles of attack. The effect of the modified fence on the slopes of the curves of figure 4(b), however, was small and inconsistent with increasing angle of attack.

The variation of control hinge-moment coefficient with angle of attack for the full-chord fence and modified fence configurations, as compared to the basic configuration, is shown in figure 5. It is apparent from figure 5 that, for the angle-of-attack range of the tests, the fences generally result in an increased linearity in the curves of control hinge-moment coefficient with angle of attack.

Slope parameters.- In reference 3, it was found that changes in the tip-control plan form without altering the basic wing plan form resulted in a linear variation of C_{h_δ} and C_{h_α} (taken at α and $\delta = 0^\circ$) with the ratio of control surface area ahead of the hinge line to total control surface area. Figure 6 shows how the addition of the fences to the basic configuration affected the slope parameters obtained at α and $\delta = 0^\circ$ as related to the correlation from reference 3.

The addition of the modified fence had little effect on the value of C_{h_δ} but the use of the full-chord fence resulted in a negative increase in this parameter. The full-chord fence of reference 1 had little effect on C_{h_δ} as shown in figure 6(a). In the case of C_{h_α} the addition of the fences (fig. 6(b)) caused appreciable negative increases in the control hinge-moment coefficients due to angle of attack. The same effect of the fence was found on the value of C_{h_α} from the tests of reference 1, which are shown in figure 6. From this preliminary investigation, it appears that the addition of fences at the wing-control juncture will not appreciably affect the correlation of C_{h_δ} but will cause basic flow changes which make it impossible to predict C_{h_α} on the basis of the correlation of reference 3.

Comparison with theory.- Theoretically, the aerodynamic characteristics of a tip control with a fence installed at the wing-control juncture will be dependent upon the relative size of the fence. If the fence is sufficiently large to isolate effectively the control from the rest of the wing, then the theoretical values of C_{h_α} and C_{h_δ} are the same as the theoretical value of C_{h_δ} for an isolated control (shown in fig. 6 as theoretical large fence). If the fence is small enough simply to seal the gap between the wing and control without protruding beyond the surfaces then the theoretical values of C_{h_α} and C_{h_δ} will be the theoretical values calculated by linear theory for the case of a control without a fence (shown in fig. 6 as theoretical basic configuration).

Figure 6(a) shows that the modified fence had little effect on C_{h_δ} but the use of the full-chord fence resulted in an increase in the negative value of C_{h_δ} which brings it close to the linearized-theory value for the basic configuration. The effect of both fences on C_{h_α} (fig. 6(b)) was to increase the basic control value beyond the theoretical large fence value and toward the theoretical value for the basic configuration. In this respect, the results of the present investigation differ from those of reference 1 where it was found that a smaller fence produced values of C_{h_α} closer to the linearized-theory value for the isolated control configuration. However, the results are similar in another respect, in that in both investigations chordwise fences had relatively little effect on C_{h_δ} but caused an increase in the negative direction in C_{h_α}.

Effect of Tabs

Hinge moments.- The variation of control hinge-moment coefficient with control deflection for the various tab configurations tested is presented in figure 7 (coefficients are based on basic control area and mean aerodynamic chord). In general, the curves are all fairly linear and parallel to one another except for the curves at 12° angle of attack which become nonlinear for positive control deflections.

Deflecting the large tab from 1.1° to -19.3° has essentially no effect on the slopes of the curves of hinge-moment coefficient with control deflection as is expected on the basis of linear theory. The effect of reducing the tab chord (figs. 7(b) to 7(d)) is to reduce the slopes of the curves, since effectively the hinge-moment-producing area is diminished while the control area and mean aerodynamic chord on which the hinge-moment coefficient is based is held constant.

The effect of angle of attack on the hinge-moment coefficient for the tab configurations tested is shown in figure 8. Here again, as the tab deflection is increased from 1.1° to -19.3°, the slopes of the curves remain constant, the curves merely shifting uniformly with increasing tab deflection as predicted by linear theory. Reducing the chord of the tab (figs. 8(d) and 8(b)) decreases the slopes of the curves of hinge-moment coefficient with angle of attack.

In order to get some evaluation of the attached tabs as a device for balancing the control hinge moments, cross plots of the variation of control hinge-moment coefficient with tab deflection for the two sizes of tabs were made from the data of figures 7 and 8. From these cross plots and from the plots of figure 7, values of $C_{h_{\delta_T}}$ and C_{h_δ} were obtained. The ratio of C_{h_δ} to $C_{h_{\delta_T}}$ is a measure of the tab deflection required

to reduce the control hinge moment per degree of control deflection to zero.

This ratio of tab deflection to control deflection required for $C_{h_\delta} = 0$ is plotted in figure 9 as a function of angle of attack for the two sizes of tabs tested herein. The curve for the small tab configuration should be considered somewhat qualitative because of the inaccuracies in determining $C_{h_{\delta_T}}$ for this configuration on the basis of only two tab deflections (one tab deflection in tests, but two in cross plots because both positive and negative angles of attack and control deflection were investigated). From figure 9, it can be seen that the small tab required very large ratios of δ_T/δ for trimming out the control hinge moment throughout the angle-of-attack range. Even the large tab required a sufficiently large ratio to discourage its use as a geared or servo tab except if relatively low maximum control deflections are permissible. At 0° angle of attack, the small tab required a range of δ_T/δ ratio 3.3 times greater than did the large tab although the area ratio of the large tab to the small tab is only 2.3:1. As the angle of attack is increased to 12°, the relative effectiveness of the tabs in reducing the control hinge moments becomes more proportional to the area ratio. The relatively large loss in effectiveness of the small tab as compared with the large tab at small angles of attack probably results from the fact that the viscous effects near the control trailing edge (shock—boundary-layer interaction, boundary-layer separation) remain relatively fixed in magnitude as the tab chord is decreased and, consequently, a larger proportion of the small tab is adversely affected. At higher angles of attack, the upper surfaces of both tabs are probably affected by separated flow, but the lower surfaces have emerged into the main airstream. (Note that $C_{h_{\delta_T}}$ was obtained at $\delta_T = 0^\circ$.) Inasmuch as the flow conditions are then probably very similar for both tabs, the tab effectiveness is proportional to their area.

Slope parameters.- The effect of the tabs on the correlation of C_{h_δ} and C_{h_α} with the correlation curves established in reference 3 is shown in figure 10. In order to make the comparison the parameters were computed by assuming that the tab was an integral part of the control (including control area and mean aerodynamic chord) and that the tab angle was fixed. For the range of tab deflections investigated on the large tab the angle at which the tab was set had no noticeable effect on C_{h_δ} or C_{h_α}. This independence of C_{h_δ} and C_{h_α} of δ_T was assumed to hold for the small tab for which no results with near 0° tab setting were obtained.

The results indicate that the effect of both large and small tabs on C_{h_δ} was to make it more negative without seriously affecting the

correlation. In the case of C_{h_α} the use of the small tabs again slightly decreased the value of the slope parameter as compared to the basic control without greatly affecting the correlation. The use of the large tab, however, resulted in such a large decrease in C_{h_α} as to make the correlation of questionable value. It should be noted, nevertheless, that nearly half the discrepancy between the correlation curve and the value of C_{h_α} for the control with the large tab is due to the basic control itself; hence, the correlation may still hold for the same tab installed on one of the other tip-control plan forms reported in reference 3.

Comparison with theory.- A comparison of the increments in hinge-moment slope parameters $\Delta C_{h_{\delta_T}}$, ΔC_{h_δ}, and ΔC_{h_α} with those predicted for the tabs by linearized supersonic theory or by some approximate expressions derived on the basis of linearized theory (see appendix) is presented in table I. Two sets of approximate equations were used to obtain ΔC_{h_δ} and ΔC_{h_α}. One set of equations involved the use of weighting factors based on the ratio of actual tab area to full-span tab area (full control or wing span depending upon parameter involved) and on the ratio of average pressure across the tab to average pressure across the control or wing span (again depending upon parameter involved). The other set of equations omitted the weighting factors based on average pressures. Experimental values of the hinge-moment parameters for the small tab were obtained by assuming that the effects of changes of tab, control, and wing deflection could be isolated as in linear theory. Tests on the large tab confirmed this assumption.

The comparison indicates that the experimental values of $\Delta C_{h_{\delta_T}}$ were considerably smaller than those predicted by linear theory with the agreement for the small tab being the poorest. These discrepancies between theory and experiment may be explained by the fact that the tabs operate in a relatively thick boundary layer off the wing. Since the small tab has a very small chord the viscous effects are proportionally larger for this tab.

In the case of ΔC_{h_δ}, the experimental values were considerably higher than the theoretical ones obtained with both weighting factors and in fairly good agreement with the theoretical values obtained by omitting the pressure weighting factor. The large difference in theoretical values is due to strong influence of tab location across the control span when the pressure weighting factor is used.

In the case of ΔC_{h_α}, the experimental values are in even poorer agreement with the theoretical results, the experimental values again

being larger. The difference between the theoretical values in this instance is smaller than in the case of ΔC_{h_δ} because of the relative location of the tab on the wing span. Since the theoretical values obtained with the use of both area and pressure weighting factors are not expected to differ by any large amount from those that would be predicted by exact linearized theory it may be concluded that exact linear theory without accounting for viscous effects cannot be used to predict theoretically the supersonic speed characteristics of the type of tabs covered in this investigation.

CONCLUSIONS

An investigation has been made at a Mach number of 1.61 and a Reynolds number of 4.2×10^6 of the effects of chordwise fences and attached tabs on the hinge-moment characteristics of a half-delta tip control mounted on a 60° delta wing. Tests were made over an angle-of-attack range from -12° to 12° and a control-deflection range from -30° to 30°. Analysis of the results indicates the following:

1. In general, the effect of fences was to improve the linearity of the hinge-moment curves and to increase the negative values of the slope parameters C_{h_δ} and C_{h_α}. The full-chord fence had a greater effect on the slope parameters than did the smaller modified fence.

2. Only the large tab had sufficient effectiveness in reducing control hinge moments to be of practical use and then only when relatively small maximum control deflections are permissible.

3. Approximate theoretical calculations, based on linear theory without accounting for viscous effects, of the control hinge-moment coefficients due to the tabs, were unsuccessful in predicting the experimental results.

Langley Aeronautical Laboratory,
National Advisory Committee for Aeronautics,
Langley Field, Va.

APPENDIX

DERIVATIONS AND FORMULAS FOR $\Delta C_{h_{\delta_T}}$, ΔC_{h_δ}, AND ΔC_{h_α}

According to linearized supersonic theory, the increment in control hinge moment due to a trailing-edge tab may be considered to be made up of three parts: the increment in control hinge moment due to tab deflection $\Delta C_{h_{\delta_T}}$, the increment in control hinge moment due to the tab as a result of control deflection ΔC_{h_δ}, and the increment in control hinge moment due to the tab as a result of a change in angle of attack ΔC_{h_α}. The linearized theory expression for $\Delta C_{h_{\delta_T}}$ is short and, hence, is derived directly. The derivation of the exact linearized-theory expressions for ΔC_{h_δ} and ΔC_{h_α} require considerable labor; hence, in their place are derived some simpler approximate equations. Most of the quantities used in deriving the expressions are defined in the sketches of figure 11. The equations are valid only when the Mach line lies ahead of the wing leading edge.

Hinge-Moment Parameter $\Delta C_{h_{\delta_T}}$

The lift coefficient and pitching-moment coefficient about the half-chord point for an isolated rectangular wing are, respectively, (ref. 4)

$$C_{L_\alpha} = \frac{4}{\beta}\left(1 - \frac{1}{2\beta A}\right) \tag{1}$$

and

$$C_{M_{\frac{1}{2}}} = \frac{1}{3\beta^2 A} \tag{2}$$

where

$$\beta = \sqrt{M^2 - 1} \qquad A = \text{Aspect ratio}$$

and

$$\beta A \geq 1$$

Dividing equation (2) by equation (1) to obtain center-of-pressure location ahead of tab half-chord point, multiplying the result by c_t/c_f to give the distance in terms of the control chord, adding the distance from the control hinge line to the tab half-chord point (fig. 11(a)) $\frac{x_h}{c_f} + \frac{c_t}{2c_f}$, and multiplying the total expression by 3/2 give the center-of-pressure distance from the control hinge line x_{cp} in terms of the control mean aerodynamic chord as

$$\frac{x_{cp}}{\bar{c}_f} = \frac{3}{2}\left[\frac{x_h}{c_f} + \frac{c_t}{2c_f} - \frac{1}{6}\left(\frac{1}{2\beta A_t - 1}\right)\frac{c_t}{c_f}\right] \tag{3}$$

The final expression for the increment in control hinge moment due to tab deflection is then obtained by multiplying the lift, equation (1), by the ratio of tab area to control area and by the moment-arm expression of equation (3). The result is

$$\Delta C_{h_{\delta_T}} = -\frac{12}{\beta}\frac{b_t}{b_f}\frac{c_t}{c_f}\left(1 - \frac{1}{2\beta A_t}\right)\left(\frac{x_h}{c_f} + \frac{c_t}{2c_f} - \frac{1}{6}\frac{1}{2\beta A_t - 1}\frac{c_t}{c_f}\right) \tag{4}$$

Hinge-Moment Parameter ΔC_{h_δ}

The pressure distribution over one surface of a half-delta tip control is given by (ref. 5)

$$C_{p_\delta} = \frac{4}{\pi\beta}\frac{m^{3/2}}{1 + m}\sqrt{\frac{1 + t}{m - t}} \tag{5}$$

which can be integrated over the control area to give the hinge moment of the control for both surfaces as

$$C_{h_\delta} = -\frac{12\sqrt{m}}{\pi\beta(1 + m)}\left(\frac{x_h}{c_f} - \frac{1}{3}\right)\left[\sqrt{m} + (1 + m)\tan^{-1}\sqrt{m}\right] \tag{6}$$

If the hinge moment is computed for the control surface ADE (fig. 11(b)) and reduced to the area and mean aerodynamic chord of control surface ABC, the hinge moment due to the tab BCED is found by subtracting the hinge moment for control ABC from that of control ADE to be

$$C_{h_\delta} = \frac{-12}{\pi} \frac{\sqrt{m}}{\beta(1 + m)} \left[\sqrt{m} + (1 + m)\tan^{-1}\sqrt{m}\right]\left[\left(\frac{c_f + c_t}{c_f}\right)^3\left(\frac{x_h + c_t}{c_f + c_t} - \frac{1}{3}\right) - \left(\frac{x_h}{c_f} - \frac{1}{3}\right)\right] \tag{7}$$

Now the ratio of tab area FGHI to tab area BCED is

$$\frac{\text{Tab area FGHI}}{\text{Tab area BCED}} = \frac{b_t}{b_f} \frac{2c_f}{2c_f + c_t} \tag{8}$$

and the ratio of average pressure across the tab FGHI to the average pressure across the tab BCED is found from

$$\frac{C_{p_{av}}\ (\text{Tab FGHI})}{C_{p_{av}}\ (\text{Tab BCED})} = \frac{\dfrac{1}{b_t}\displaystyle\int_{t_1}^{t_2} \frac{4}{\beta} \frac{m^{3/2}}{1 + m}\sqrt{\frac{1 + t}{m - t}}\, dt}{\dfrac{2}{b_f + b_f \dfrac{c_f + c_t}{c_f}}\displaystyle\int_0^m \frac{4}{\beta} \frac{m^{3/2}}{1 + m}\sqrt{\frac{1 + t}{m - t}}\, dt}$$

to be

$$\frac{C_{p_{av}}\ (\text{Tab FGHI})}{C_{p_{av}}\ (\text{Tab BCED})} = \frac{b_f}{b_t}\,\frac{2c_f + C_t}{2c_f}\left\{\frac{\sqrt{m - t_1}\,\sqrt{1 + t_1} - \sqrt{m - t_2}\,\sqrt{1 + t_2} + \frac{m + 1}{2}K}{\sqrt{m} + \frac{m + 1}{2}\left[\sin^{-1}\left(\frac{m - 1}{m + 1}\right) - \frac{\pi}{2}\right]}\right\} \tag{9}$$

where

$$K = \sin^{-1}\left(\frac{m - 1 - 2t_2}{m + 1}\right) - \sin^{-1}\left(\frac{m - 1 - 2t_1}{m + 1}\right)$$

In order to obtain the final equation for ΔC_{h_δ}, equation (7) is multiplied by the area ratio of equation (8) and the average pressure ratio of equation (9). The final result is

$$\Delta C_{h_\delta} = -\frac{12}{\pi}\,\frac{\sqrt{m}}{\beta(1 + m)}\left[\sqrt{m} + (1 + m)\tan^{-1}\sqrt{m}\right]\left[\left(\frac{c_f + c_t}{c_f}\right)^3\left(\frac{x_h + c_t}{c_f + c_t} - \frac{1}{3}\right) - \left(\frac{x_h}{c_f} - \frac{1}{3}\right)\right]\left\{\frac{\sqrt{m - t_1}\,\sqrt{1 + t_1} - \sqrt{m - t_2}\,\sqrt{1 + t_2} + \frac{m + 1}{2}\left[\sin^{-1}\left(\frac{m - 1 - 2t_2}{m + 1}\right) - \sin^{-1}\left(\frac{m - 1 - 2t_1}{m + 1}\right)\right]}{\sqrt{m} + \frac{m + 1}{2}\left[\sin^{-1}\left(\frac{m - 1}{m + 1}\right) - \frac{\pi}{2}\right]}\right\} \tag{10}$$

If the weighting factor of average pressures (eq. (9)) is omitted, the equation for the increment in hinge moment simplifies to

$$\Delta C_{h_\delta} = -\frac{12}{\pi}\frac{\sqrt{m}}{\beta(1+m)}\left[\sqrt{m} + (1+m)\tan^{-1}\sqrt{m}\right]\left[\left(\frac{c_f + c_t}{c_f}\right)^3\left(\frac{x_h + c_t}{c_f + c_t} - \frac{1}{3}\right) - \left(\frac{x_h}{c_f} - \frac{1}{3}\right)\right]\frac{b_t}{b_f}\frac{2c_f}{2c_f + c_t} \tag{11}$$

Hinge-Moment Parameter ΔC_{h_α}

The pressure distribution over one surface of a triangular wing is given by (ref. 4)

$$C_{p_\alpha} = \frac{2m}{\beta E\left(\sqrt{1 - m^2}\right)\sqrt{1 - \frac{t^2}{m^2}}} \tag{12}$$

where $E\left(\sqrt{1 - m^2}\right)$ is a complete elliptic integral of the second kind with modulus $\sqrt{1 - m^2}$. Integration of this pressure distribution over both surfaces of the wing results in

$$C_{L_\alpha} = \frac{1}{\beta}\frac{2\pi m}{E\left(\sqrt{1 - m^2}\right)} \tag{13}$$

with the center of pressure at $2/3c_f$ from the wing apex. If the moment of wing ADE (fig. 11(c)) about the control hinge line is found and reduced to the dimensions of wing ABC, then the hinge moment due to the tab BCED is found by subtracting the moment of wing ABC about the control hinge line from that of wing ADE and converting the result from the basis of wing area ABC and wing

root chord to control area and control mean aerodynamic chord. The result is

$$\Delta C_{h_\alpha} = -\frac{3}{\beta}\frac{\pi m}{E\left(\sqrt{1 - m^2}\right)}\left(\frac{c_w}{c_f}\right)^3\left[\left(\frac{x_h + c_t}{c_w + c_t} - \frac{1}{3}\right)\left(\frac{c_w + c_t}{c_w}\right)^3 - \left(\frac{x_h}{c_w} - \frac{1}{3}\right)\right] \tag{14}$$

The ratio of area of tab FGHI to tab BCED is

$$\frac{\text{Tab area FGHI}}{\text{Tab area BCED}} = \frac{b_t}{b_w}\frac{2c_w}{2c_w + c_t} \tag{15}$$

and the average pressure over tab FGHI to average pressure over tab BCED is found from

$$\frac{C_{p_{av}}\ \text{tab FGHI}}{C_{p_{av}}\ \text{tab BCED}} = \frac{\dfrac{1}{b_t}\displaystyle\int_{t_1}^{t_2}\frac{2m}{\beta E\left(\sqrt{1 - m^2}\right)\sqrt{1 - \frac{t^2}{m^2}}}\,dt}{\dfrac{2}{b_w + b_w\left(\frac{c_w + c_t}{c_w}\right)}\displaystyle\int_0^m\frac{2m}{\beta E\left(\sqrt{1 - m^2}\right)\sqrt{1 - \frac{t^2}{m^2}}}\,dt}$$

to be

$$\frac{C_{p_{av}}\ \text{tab FGHI}}{C_{p_{av}}\ \text{tab BCED}} = \left(\frac{b_w}{b_t}\right)\left(\frac{2c_w + c_t}{2c_w}\right)\left(\frac{\sin^{-1}\frac{t_2}{m} - \sin^{-1}\frac{t_1}{m}}{\frac{\pi}{2}}\right) \tag{16}$$

In order to obtain the final equation for ΔC_{h_α}, equation (14) is multiplied by the area ratio of equation (15) and the average-pressure ratio of equation (16). The final result is

$$\Delta C_{h_\alpha} = -\frac{6}{\beta}\frac{m}{E\left(\sqrt{1 - m^2}\right)}\left(\frac{c_w}{c_f}\right)^3\left[\left(\frac{x_h + c_t}{c_w + c_t} - \frac{1}{3}\right)\left(\frac{c_w + c_t}{c_w}\right)^3 - \left(\frac{x_h}{c_w} - \frac{1}{3}\right)\right]\left(\sin^{-1}\frac{t_2}{m} - \sin^{-1}\frac{t_1}{m}\right) \tag{17}$$

If the weighting factor of average pressure is omitted, the equation changes to

$$\Delta C_{h_\alpha} = -\frac{3}{\beta}\frac{\pi m}{E\left(\sqrt{1 - m^2}\right)}\left(\frac{c_w}{c_f}\right)^3\left(\frac{b_t}{b_w}\right)\frac{2c_w}{2c_w + c_t}\left[\left(\frac{x_h + c_t}{c_w + c_t} - \frac{1}{3}\right)\left(\frac{c_w + c_t}{c_w}\right)^3 - \left(\frac{x_h}{c_w} - \frac{1}{3}\right)\right] \tag{18}$$

REFERENCES

1. Guy, Lawrence D.: Control Hinge-Moment and Effectiveness Characteristics of a 60° Half-Delta Tip Control on a 60° Delta Wing at Mach Numbers of 1.41 and 1.96. NACA RM L52H13, 1952.

2. Lockwood, Vernard E., and Fikes, Joseph E.: Preliminary Investigation at Transonic Speeds of the Effect of Balancing Tabs on the Hinge-Moment and Other Aerodynamic Characteristics of a Full-Span Flap on a Tapered 45° Sweptback Wing of Aspect Ratio 3. NACA RM L52A23, 1952.

3. Czarnecki, K. R., and Lord, Douglas R.: Hinge-Moment Characteristics for Several Tip Controls on a 60° Sweptback Delta Wing at Mach Number 1.61. NACA RM L52K28, 1953.

4. Ferri, Antonio: Elements of Aerodynamics of Supersonic Flows. The Macmillan Company, 1949.

5. Kainer, Julian H., and King, Mary Dowd: The Theoretical Characteristics of Triangular-Tip Control Surfaces at Supersonic Speeds. Mach Lines Behind Trailing Edges. NACA TN 2715, 1952.

TABLE I

COMPARISON OF THEORETICAL AND EXPERIMENTAL VALUES

OF HINGE-MOMENT PARAMETERS

Tab	Hinge-moment parameter	Experimental value	Theoretical values		
			Exact linear theory	Approximate theory with area and pressure weighting factors	Approximate theory with area weighting factors only
Large	$\Delta C_{h_{\delta_T}}$	-0.0039	-0.0048		
Small		-.0010	-.0021		
Large	$\Delta C_{h_{\delta}}$	-.0038		-0.0021	-0.0035
Small		-.0021		-.0008	-.0014
Large	$\Delta C_{h_{\alpha}}$	-.0088		-.0047	-.0045
Small		-.0046		-.0020	-.0018

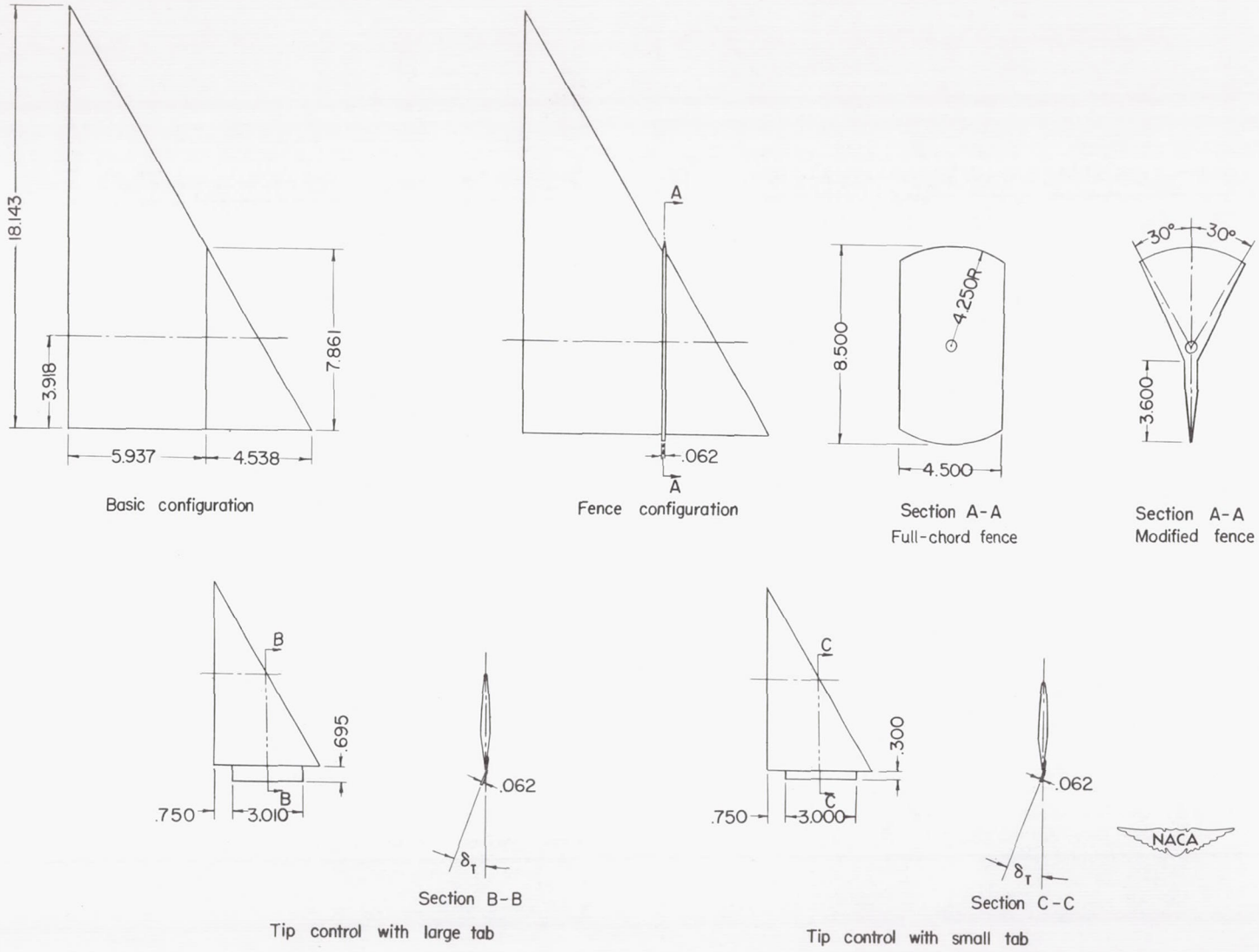

Figure 1 - Sketch of model configurations tested. All dimensions in inches.

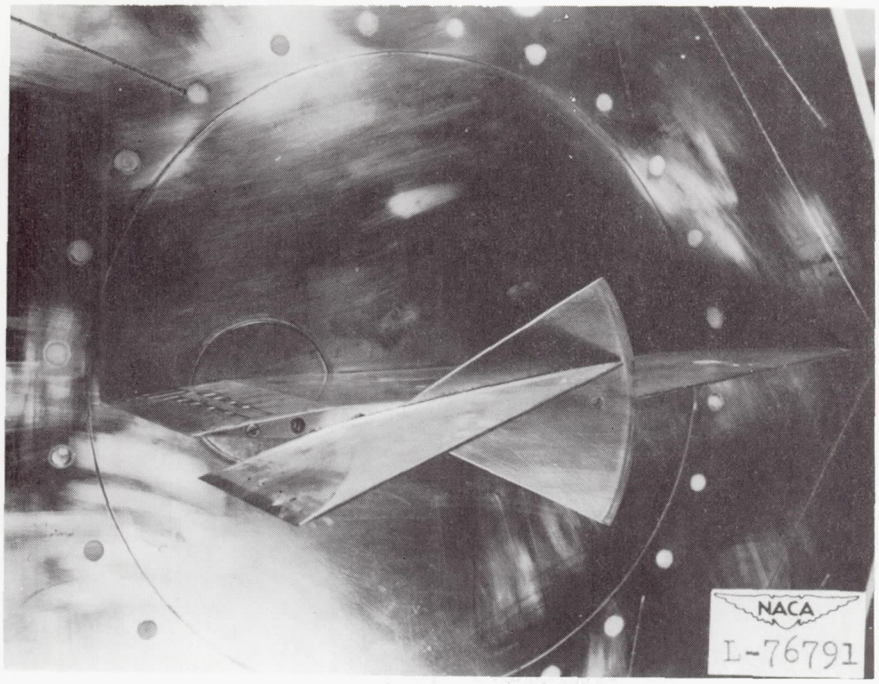

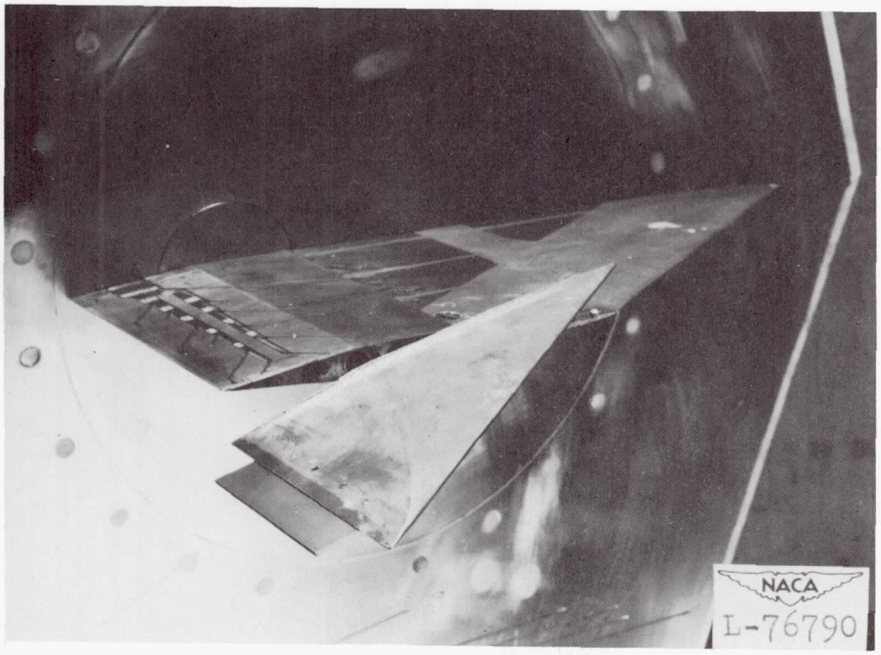

Figure 2.- Photographs of model showing modified-fence and large-tab installation.

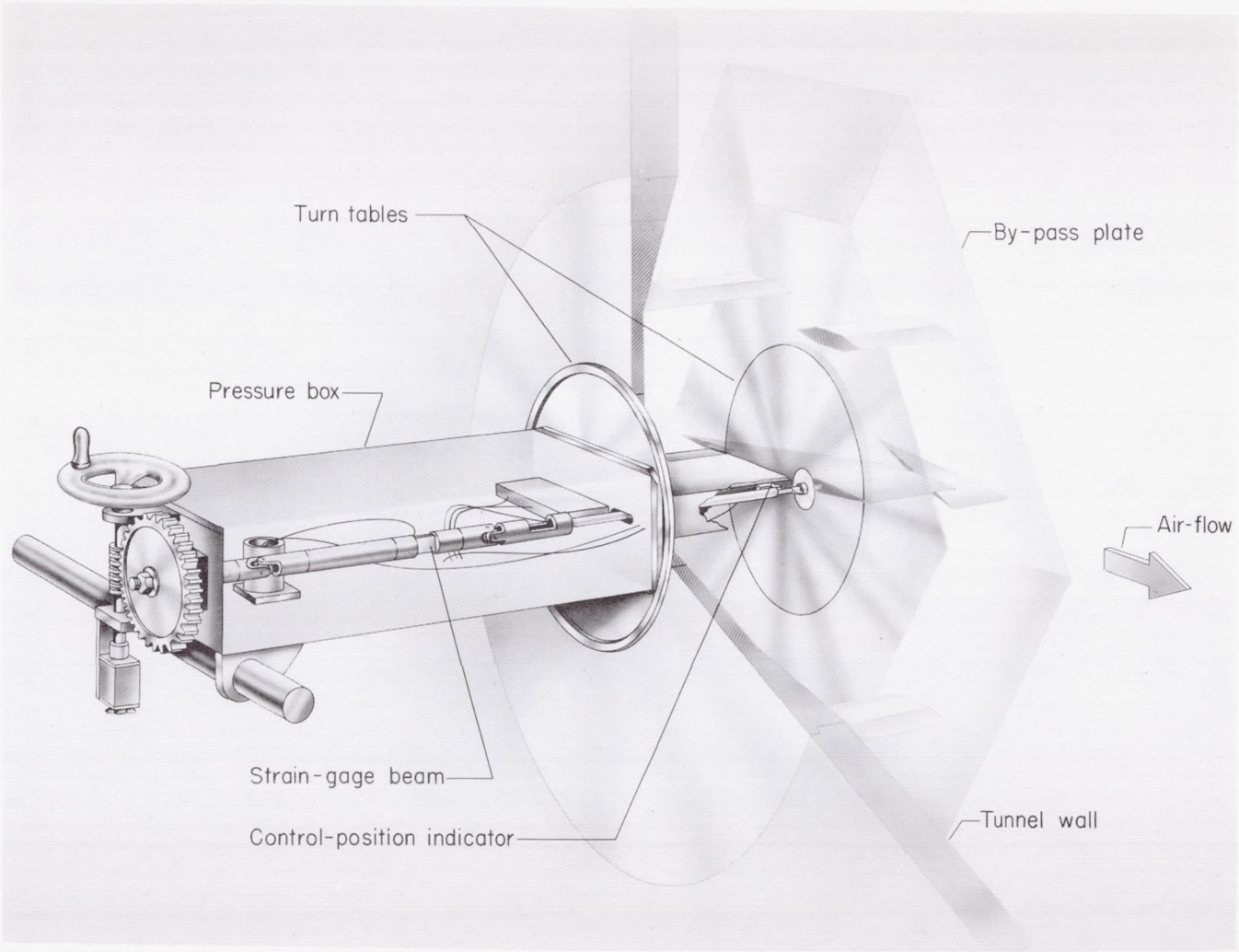

Figure 3.- Sketch of test setup.

NACA
L-77038

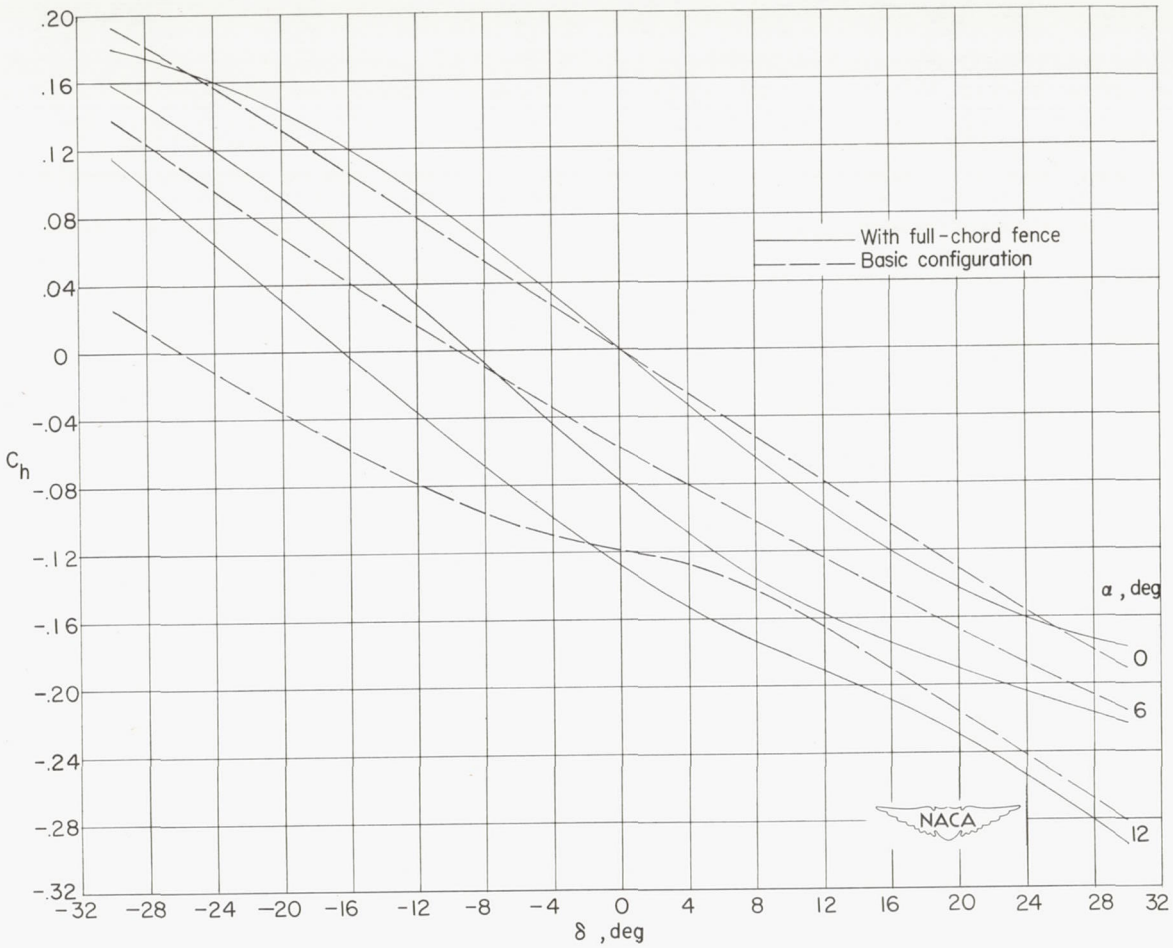

(a) With full-chord fence.

Figure 4.- Variation of control-surface hinge-moment coefficient with control deflection for the fence configurations and for the basic configuration.

CONFIDENTIAL

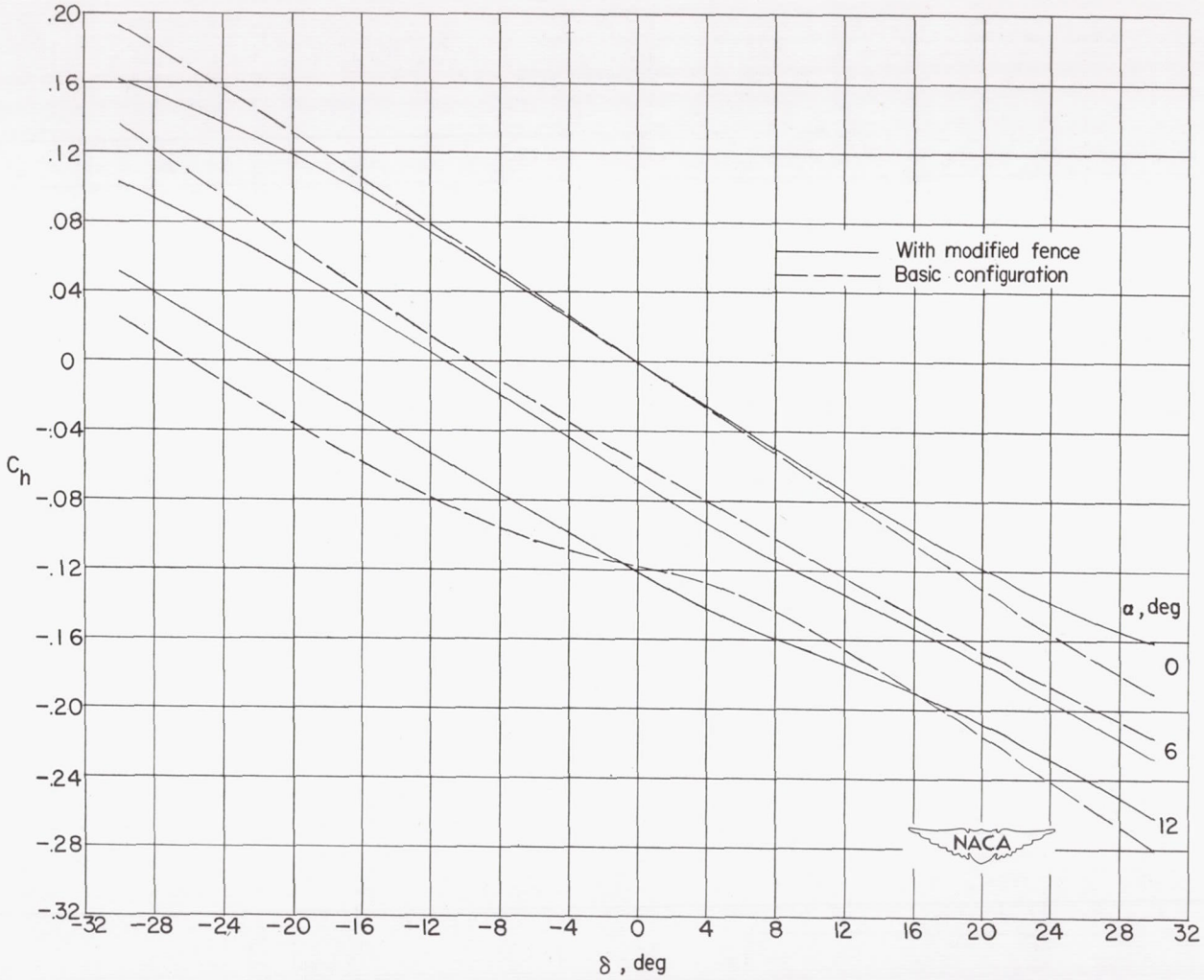

(b) With modified fence.

Figure 4.- Concluded.

CONFIDENTIAL

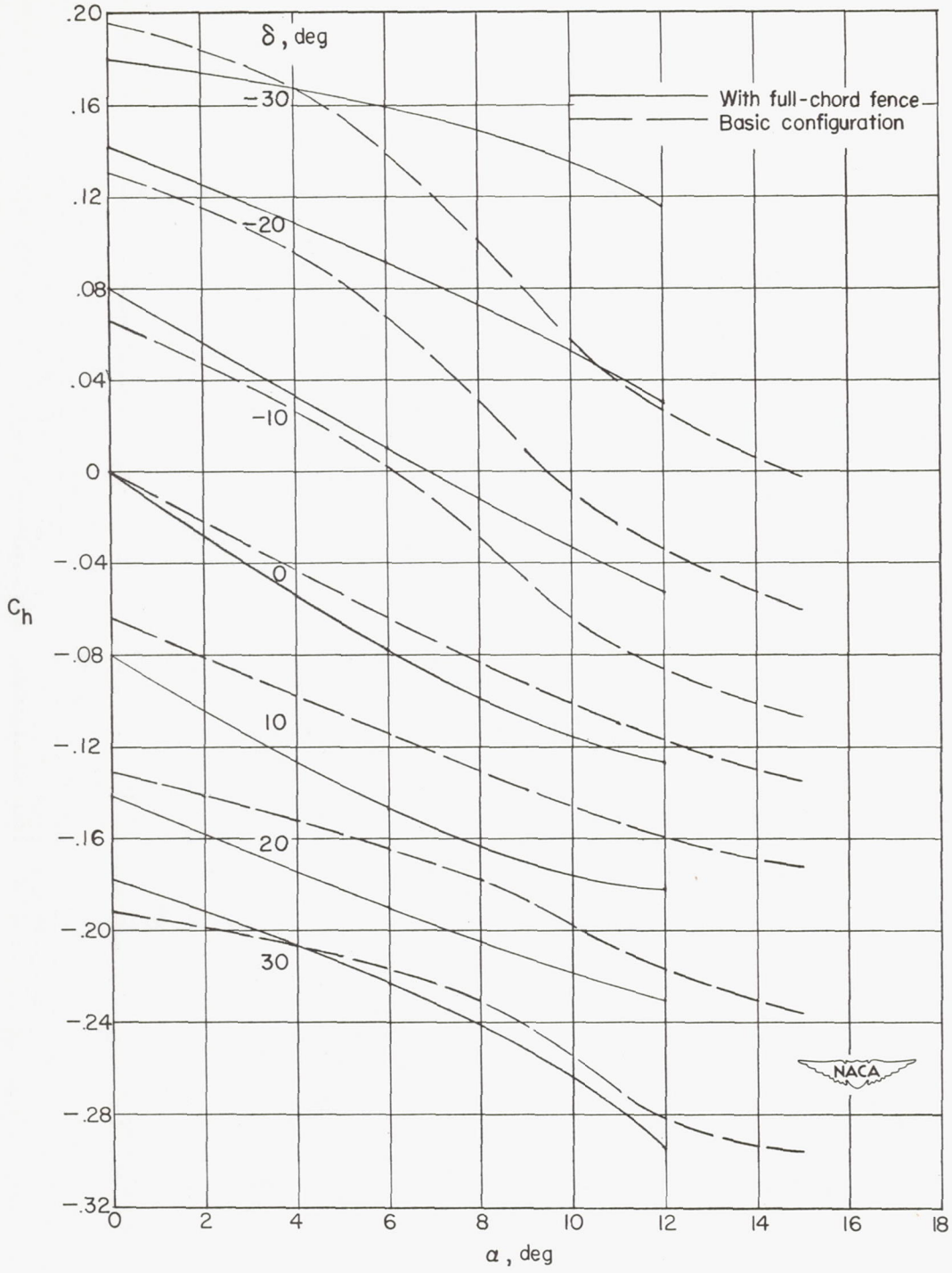

(a) With full-chord fence.

Figure 5.- Variation of control-surface hinge-moment coefficient with angle of attack for the fence configurations and for the basic configuration.

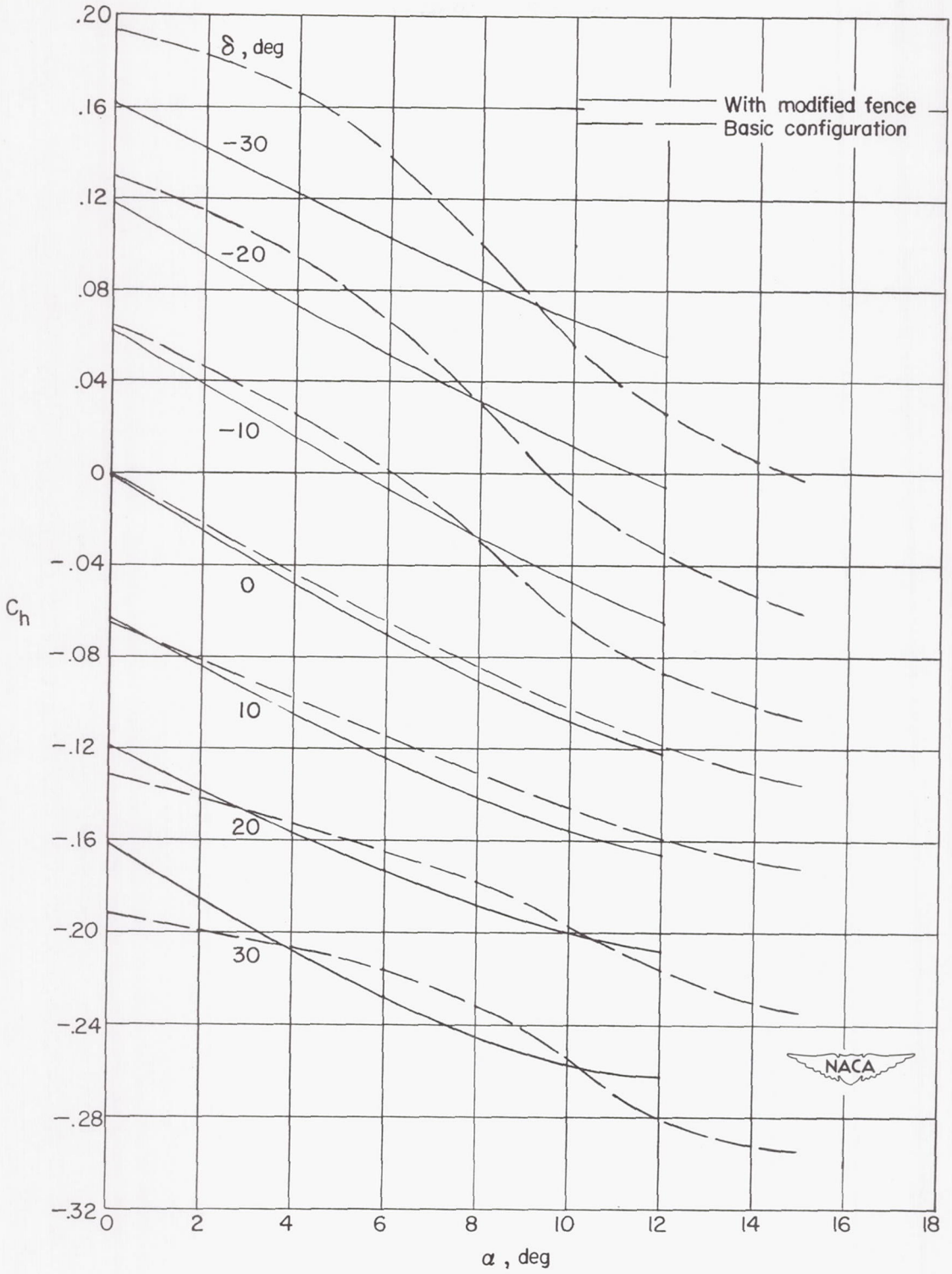

(b) With modified fence.

Figure 5.- Concluded.

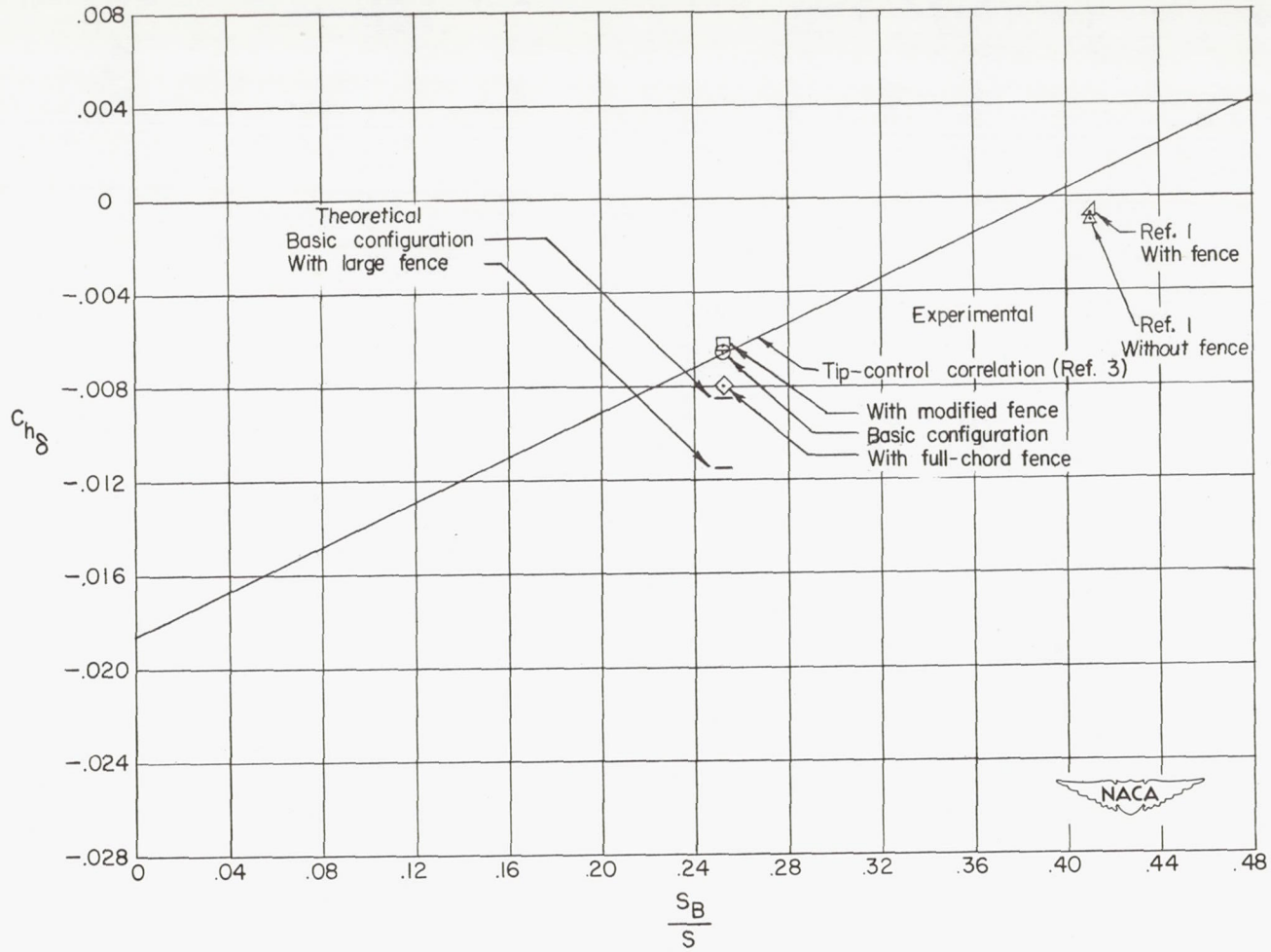

(a) C_{h_δ}.

Figure 6.- Comparison of slope parameters C_{h_δ} and C_{h_α} for fence configurations with the tip control correlation of reference 3.

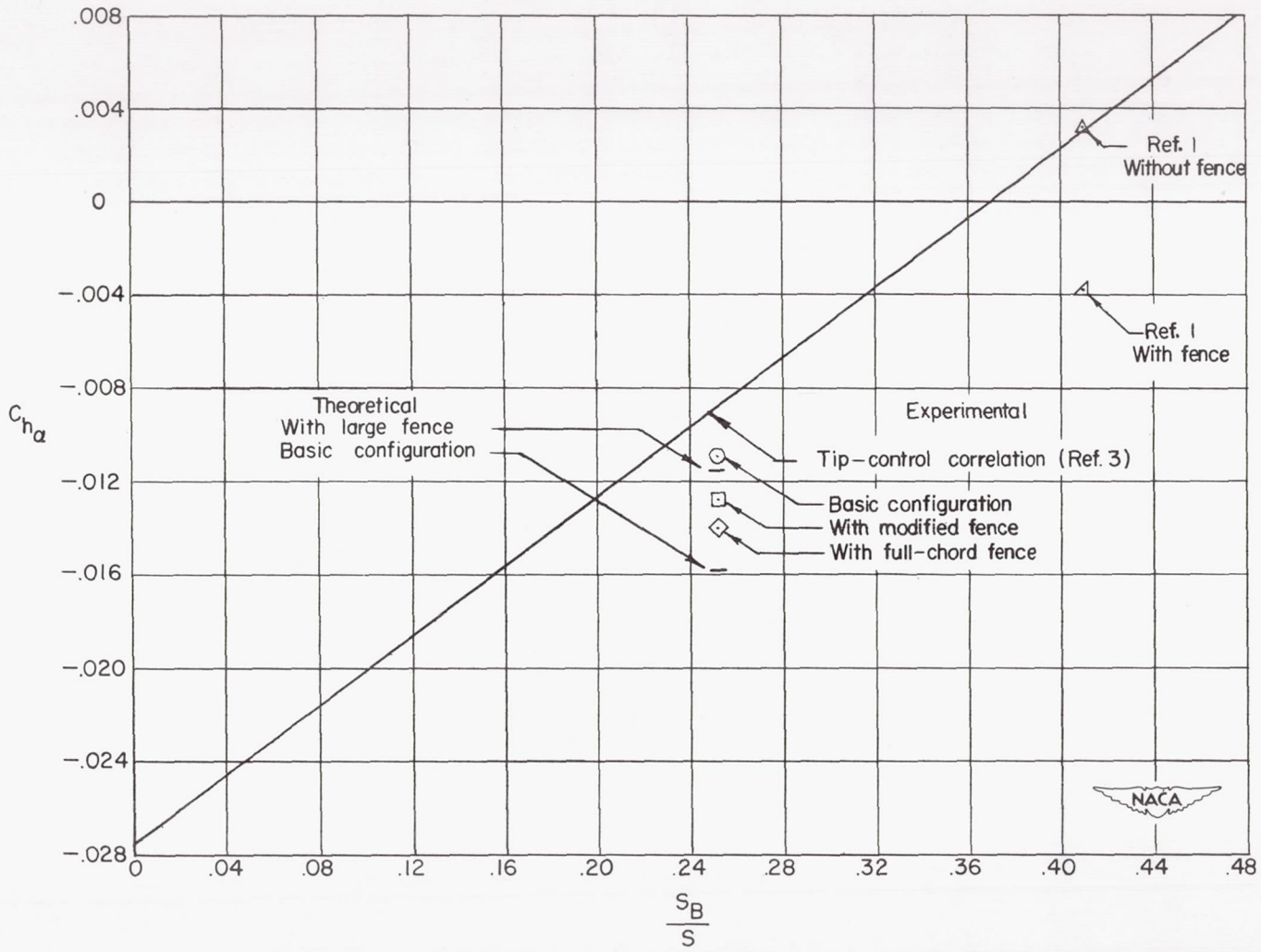

(b) C_{h_α}.

Figure 6.- Concluded.

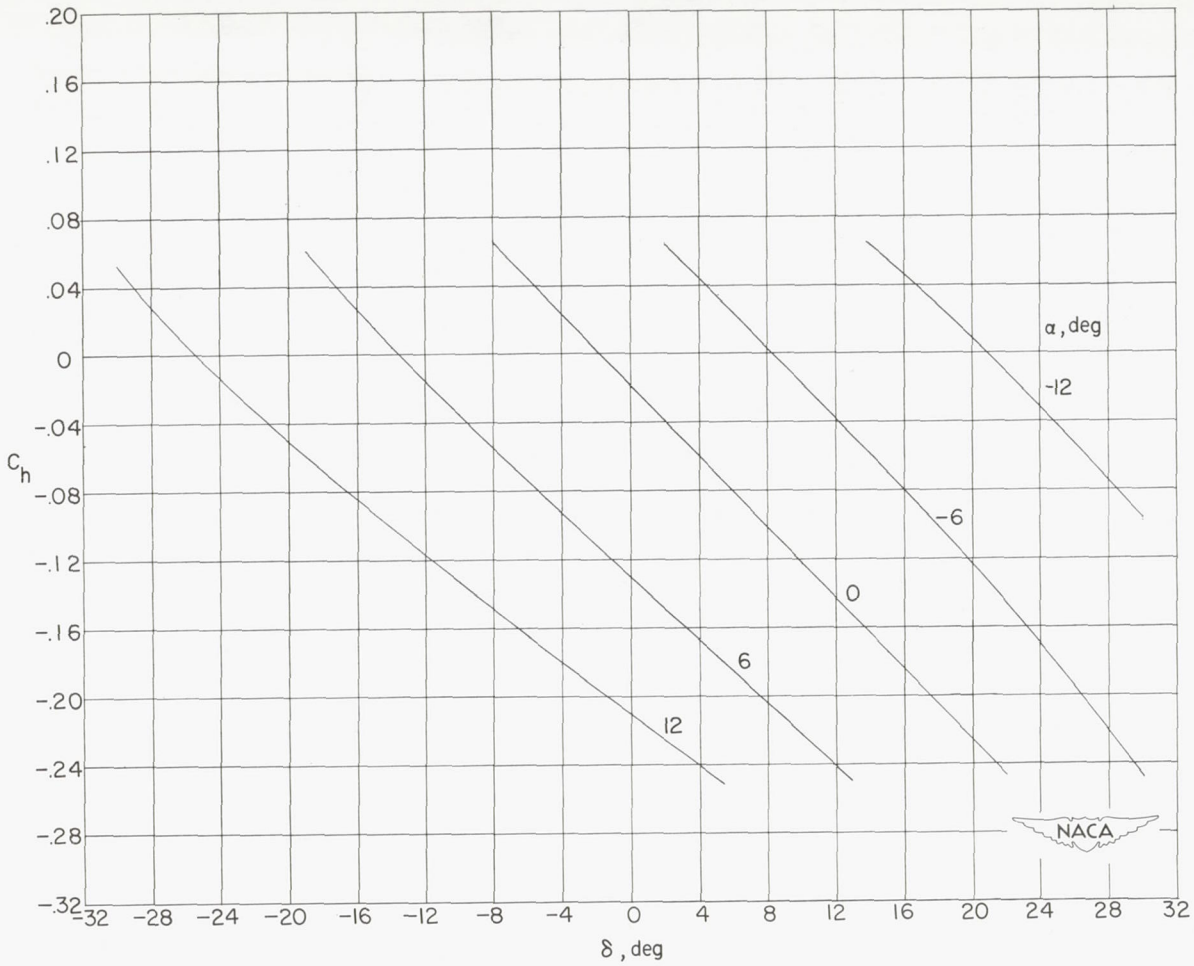

(a) Large tab, $\delta_T = 1.1^{\circ}$.

Figure 7.- Variation of control-surface hinge-moment coefficient with control deflection for the tab configurations.

(b) Large tab, $\delta_T = -9.3^{\circ}$.

Figure 7.- Continued.

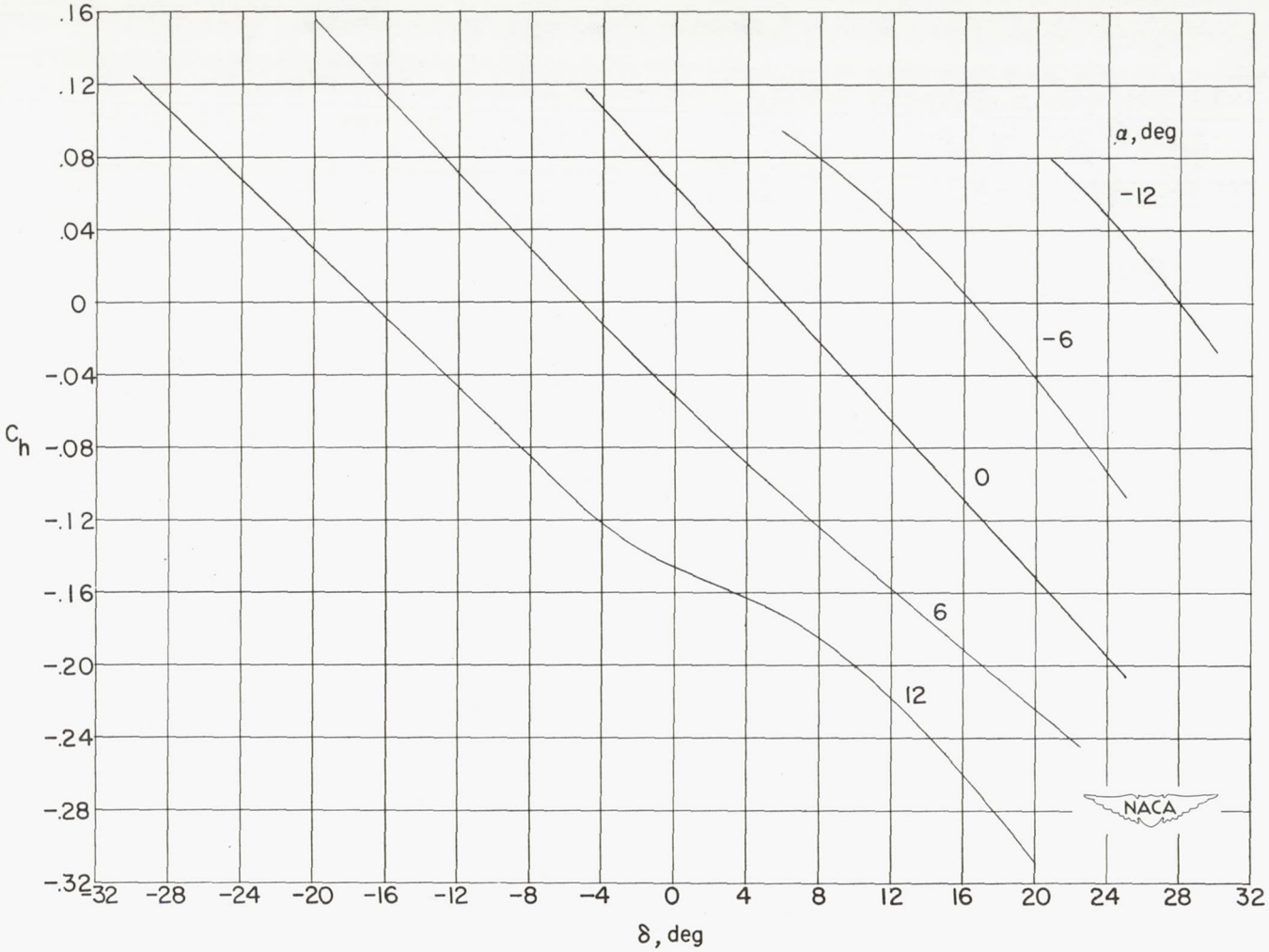

(c) Large tab, $\delta_T = -19.3^{\circ}$.

Figure 7.- Continued.

(d) Small tab, $\delta_T = -10.8^{\circ}$.

Figure 7.- Concluded.

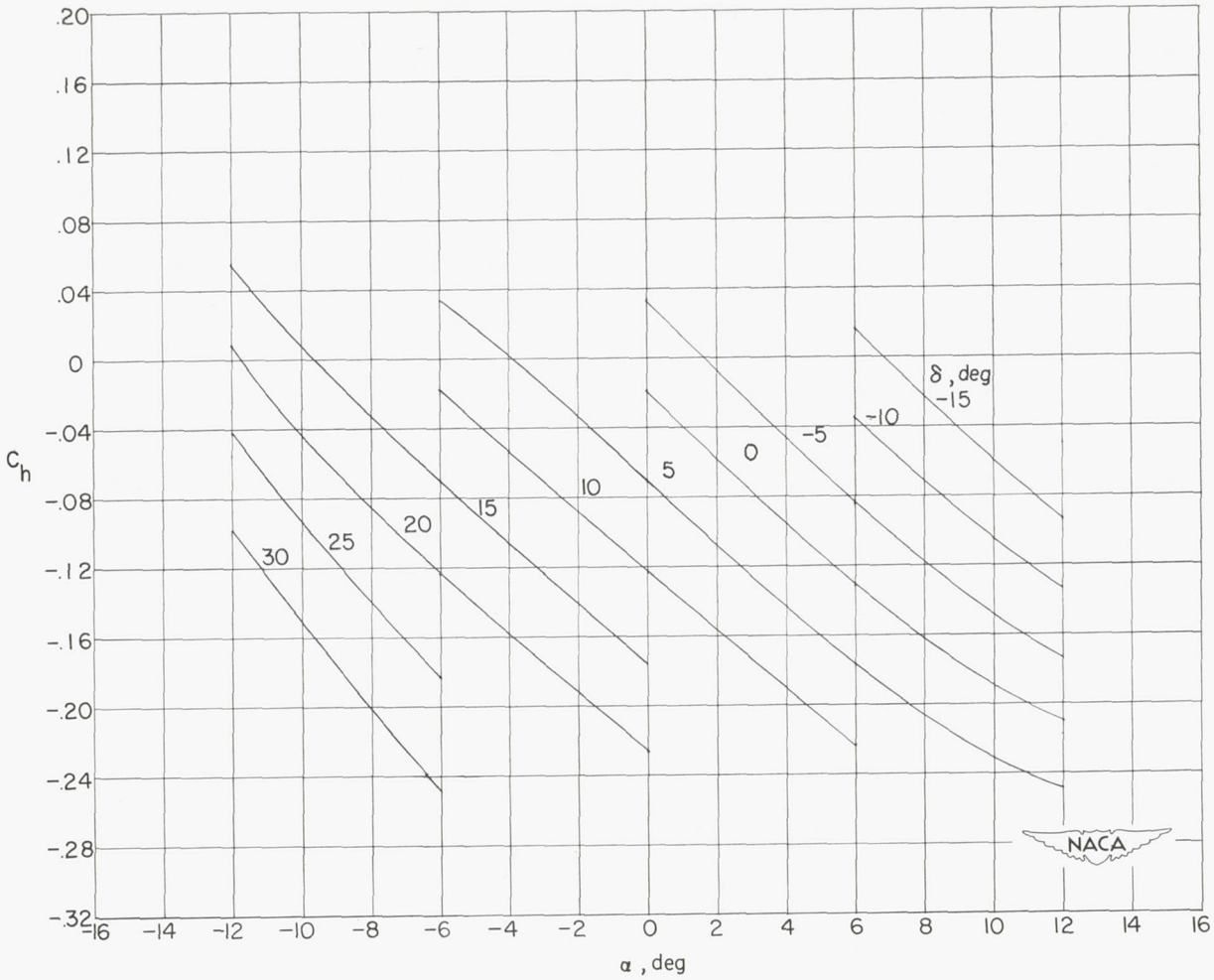

(a) Large tab, $\delta_T = 1.1^{\circ}$.

Figure 8.- Variation of control-surface hinge-moment coefficient with angle of attack for the tab configuration.

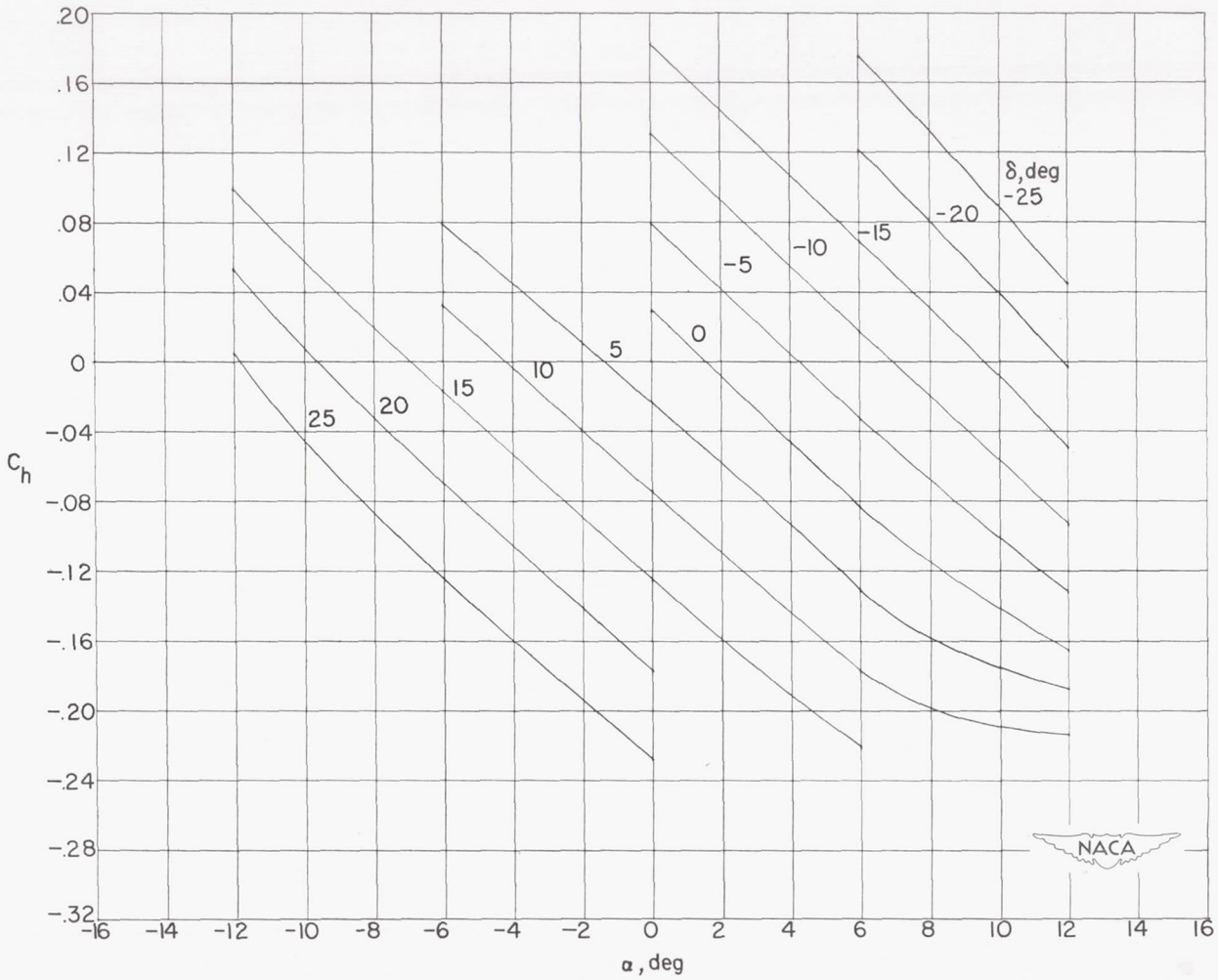

(b) Large tab, $\delta_T = -9.3^{\circ}$.

Figure 8.- Continued.

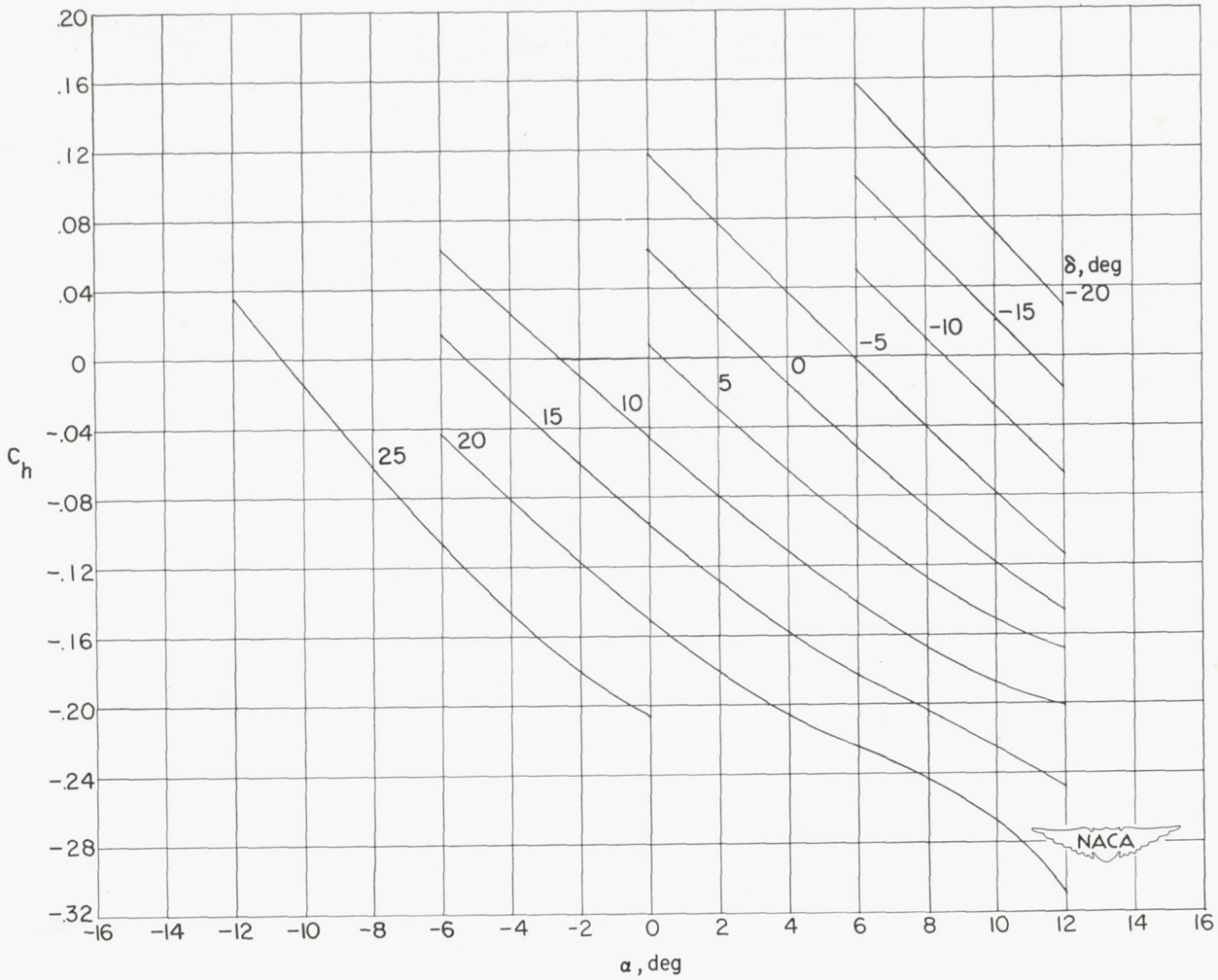

(c) Large tab, $\delta_T = -19.3^{\circ}$.

Figure 8.- Continued.

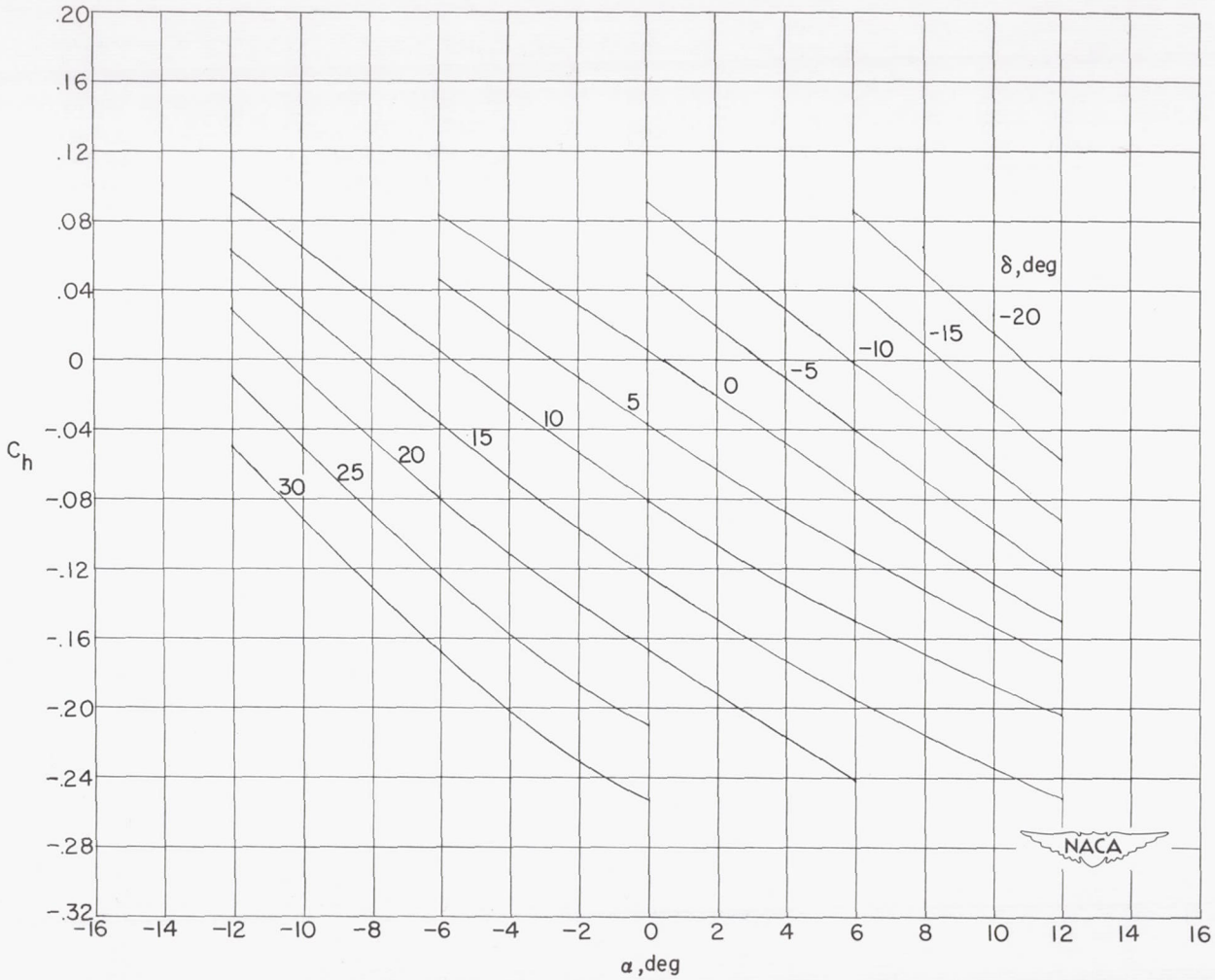

(d) Small tab, $\delta_T = -10.8^{\circ}$.

Figure 8.- Concluded.

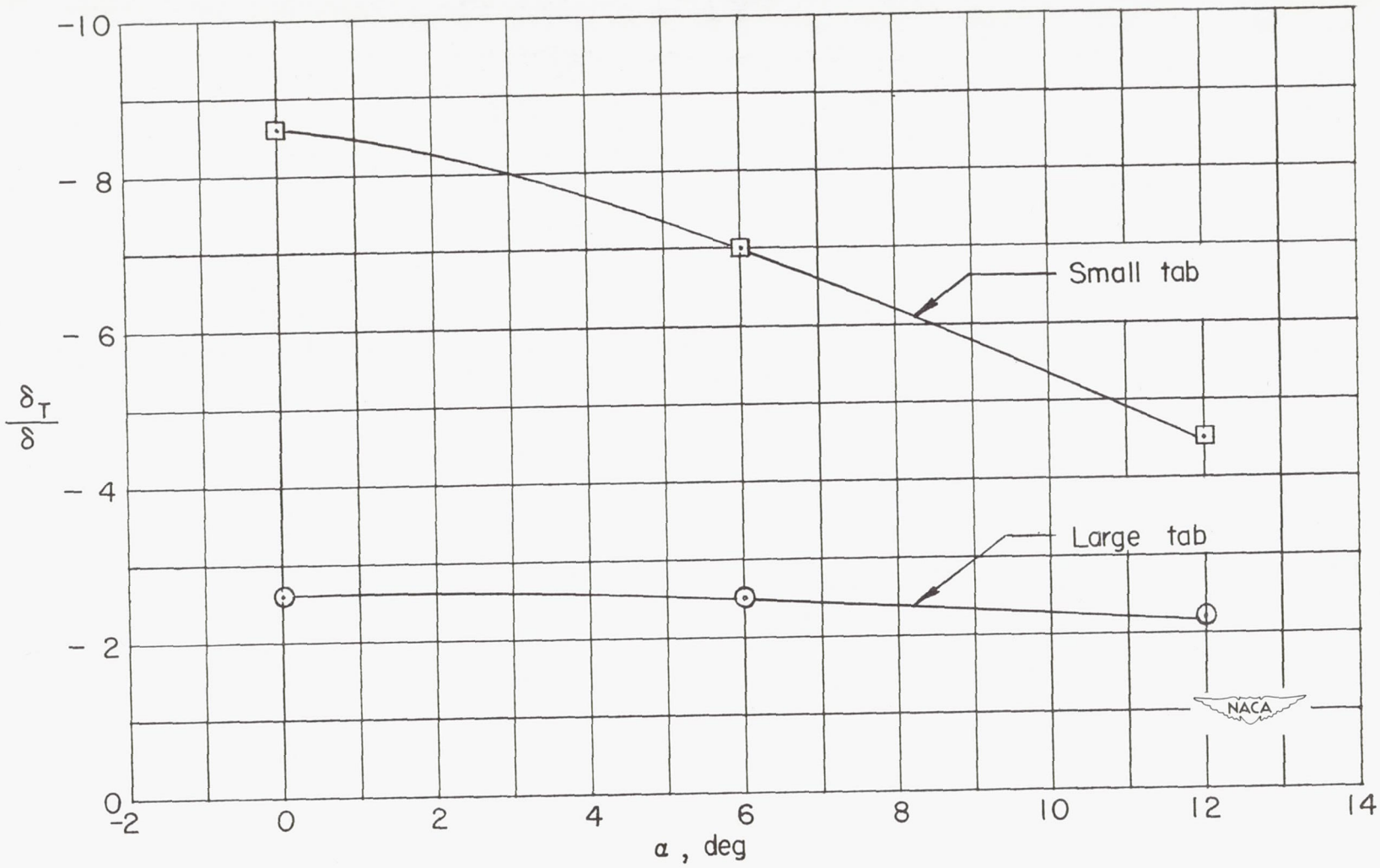

Figure 9.- Variation with angle of attack of the ratio of tab deflection to control deflection required for $C_{h_\delta} = 0$.

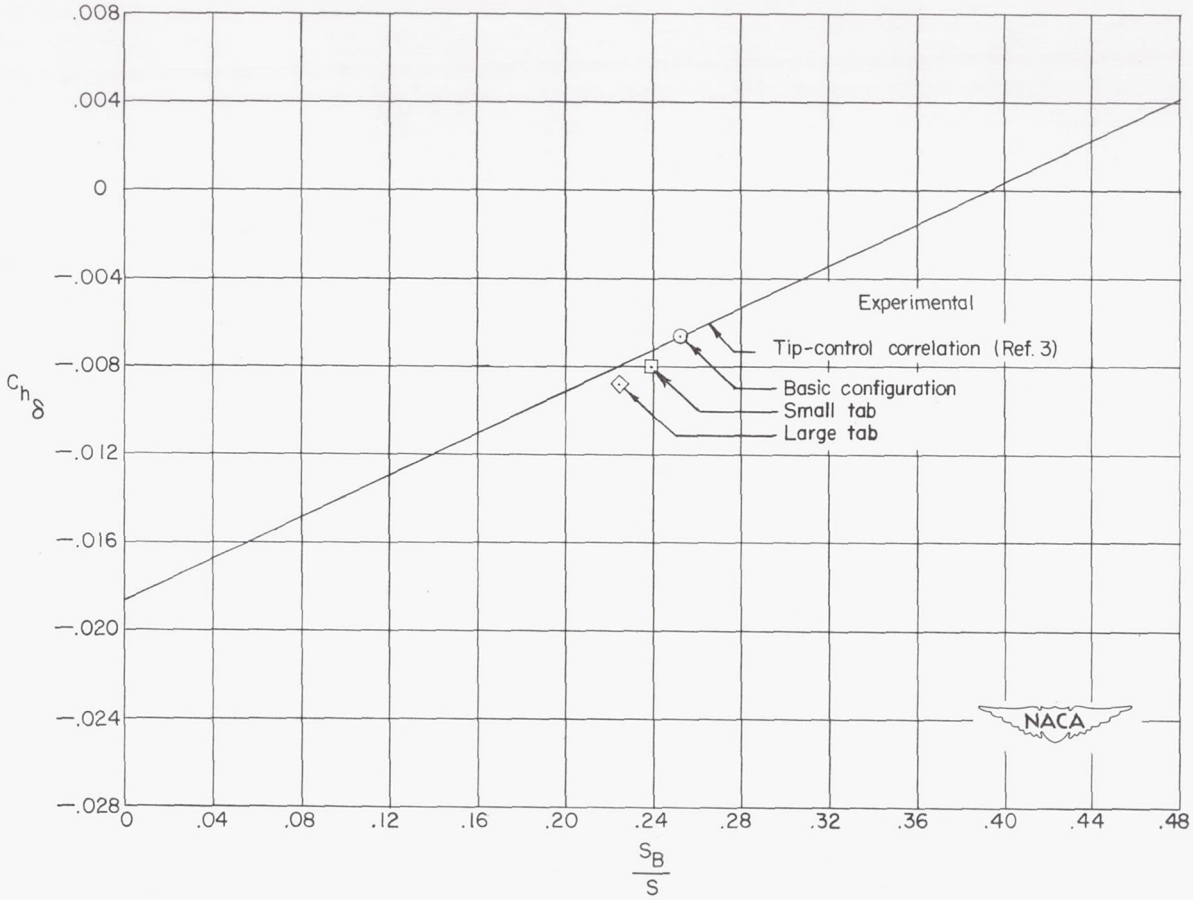

(a) C_{h_δ}.

Figure 10.- Comparison of slope parameters C_{h_δ} and C_{h_α} for tab configurations with the tip-control correlation of reference 3. Coefficients based on area and mean aerodynamic chord of control including tab area.

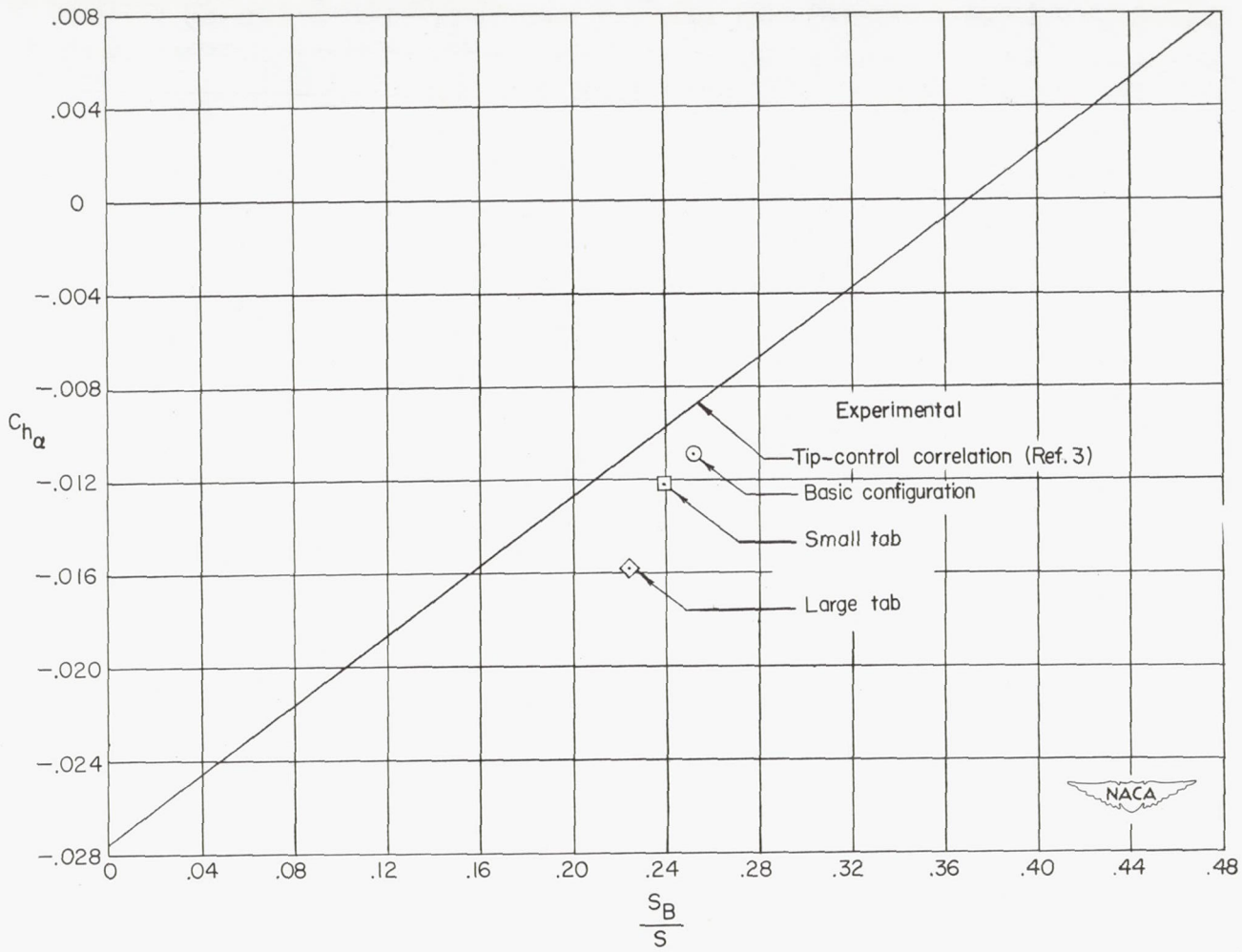

(b) C_{h_α}.

Figure 10.- Concluded.

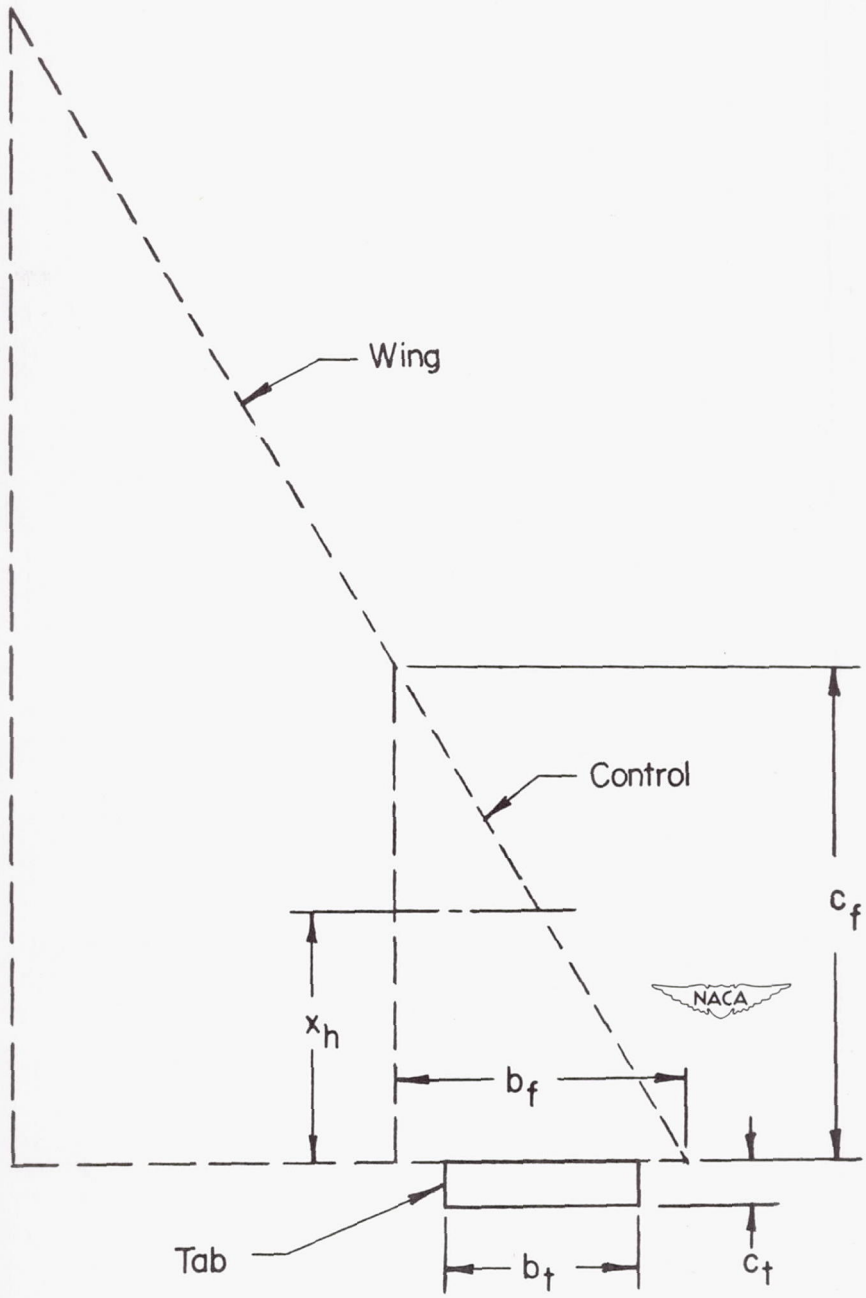

(a) $\Delta C_{h_{\delta_T}}$.

Figure 11.- Definitions of the various quantities used in deriving expressions for the increment in control hinge-moment coefficient due to the tab as a result of tab, control, and wing deflection.

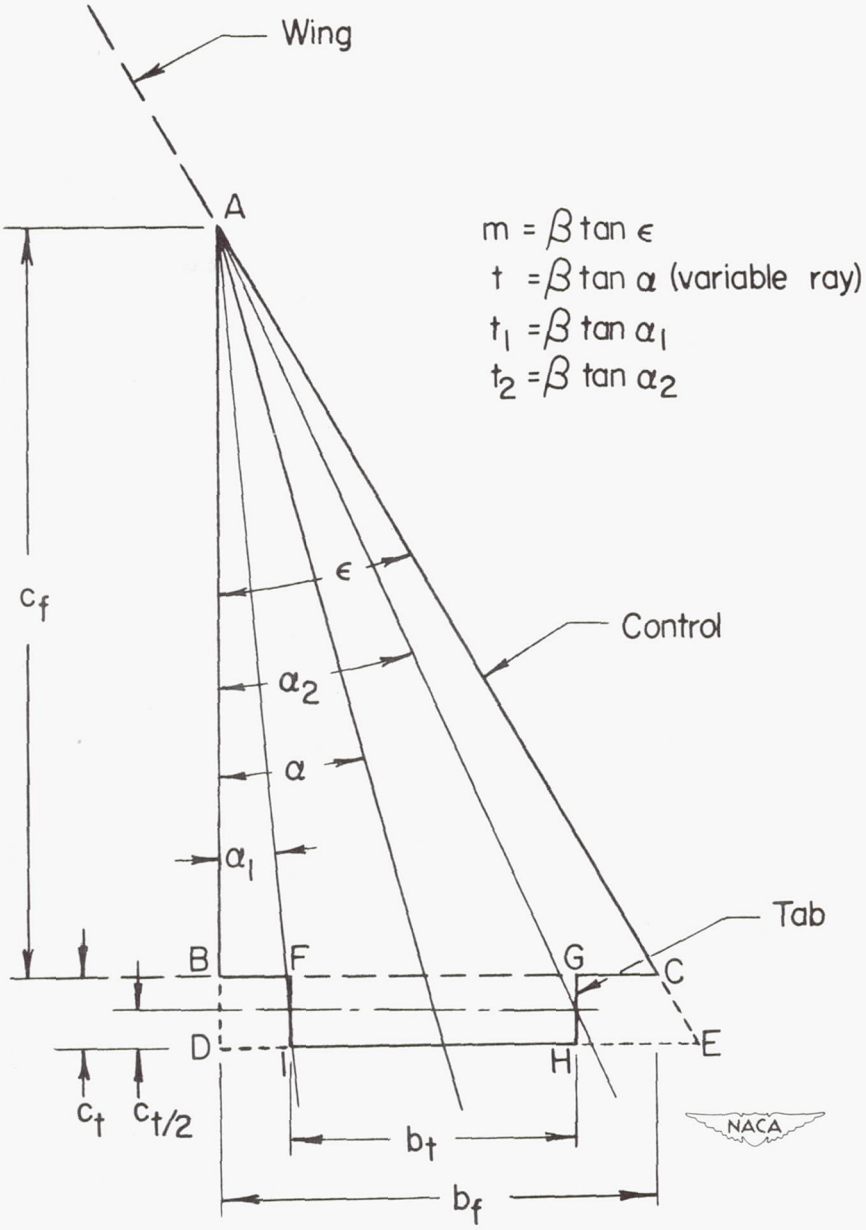

(b) ΔC_{h_δ}.

Figure 11.- Continued.

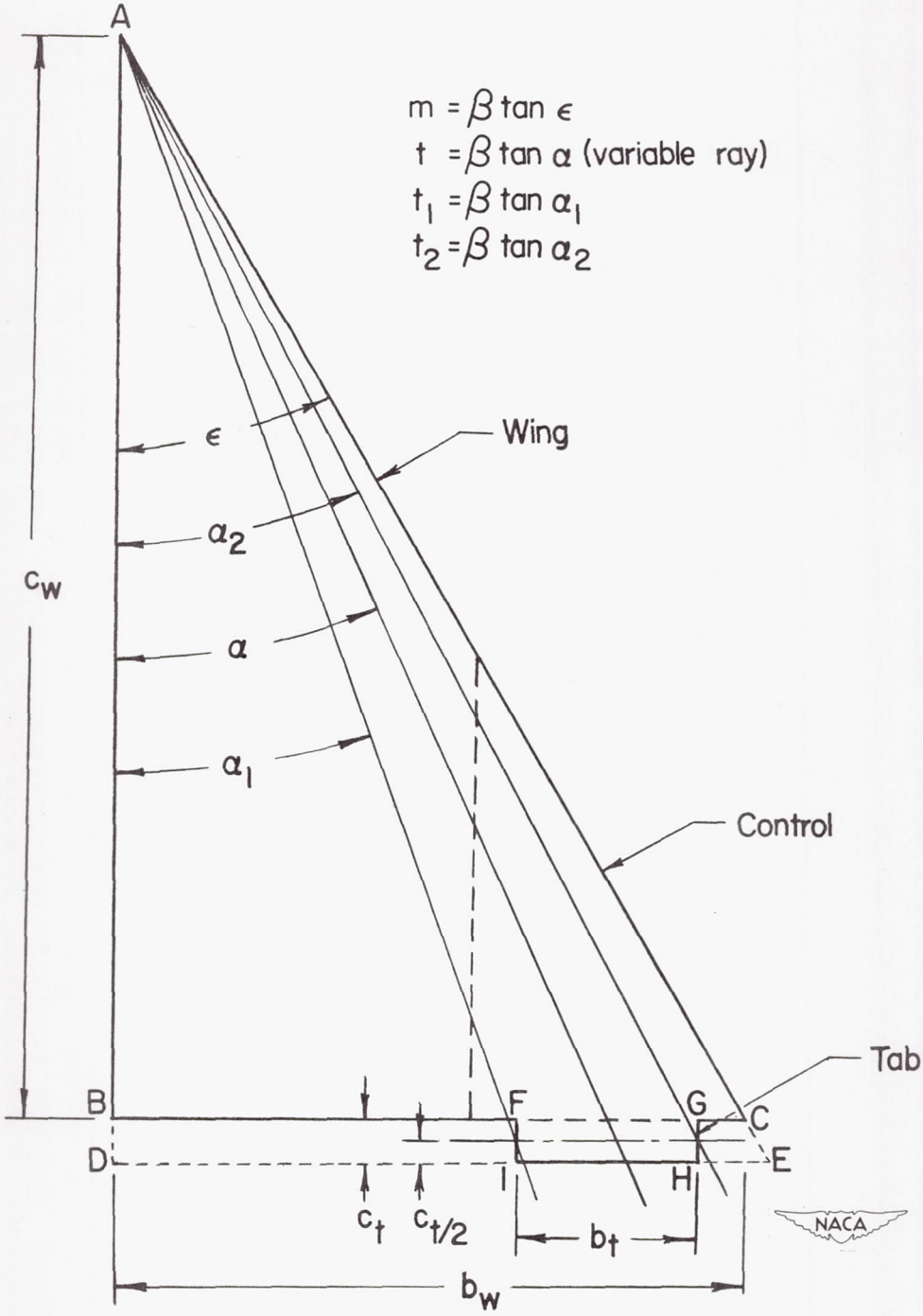

(c) ΔC_{h_α}.

Figure 11.- Concluded.

NACA-Langley - 5-29-53 - 350